IEEE Access

Received 13 April 2023, accepted 4 May 2023, date of publication 16 May 2023, date of current version 30 May 2023.

Digital Object Identifier 10.1109/ACCESS.2023.3276904

RESEARCH ARTICLE

A New Flexible Four Parameter Bathtub Curve Failure Rate Model, and Its Application to Right-Censored Data

LAILA A. AL-ESSA[1], MUSTAPHA MUHAMMAD[2], M. H. TAHIR[3], BADAMASI ABBA[4], JINSEN XIAO[2], AND FARRUKH JAMAL[3]

[1]Department of Mathematical Sciences, College of Science, Princess Nourah bint Abdulrahman University, P.O. Box 84428, Riyadh 11671, Saudi Arabia
[2]Department of Mathematics, Guangdong University of Petrochemical Technology, Maoming 525000, China
[3]Department of Statistics, The Islamia University of Bahawalpur (IUB), Bahawalpur, Punjab 63100, Pakistan
[4]School of Mathematics and Statistics, Central South University, Hunan 410083, China

Corresponding author: Farrukh Jamal (farrukh.jamal@iub.edu.pk)

ABSTRACT This article introduces a new flexible four parameter distribution by convolution of the exponential and Weibull distribution using the odd function transformation, which offers greater flexibility in terms of fit, its called the modified exponential-Weibull (MEW). The MEW model is designed to provide a more accurate description of failure time data resulting from a system with one or more failure modes and is characterized by a hazard rate (HR) that takes the shape of a bathtub due to its complexity. The moments properties, quantile function, and residual life are derived and discussed. We discussed the HR function and several distributional properties of the MEW model, and applied maximum likelihood and Bayesian techniques to estimate its unknown parameters. The Hamiltonian Monte Carlo (HMC) algorithm is employed to simulate the posterior distributions and verify the MEW Bayes estimators. We examined the behavior of the MEW model on two data sets with bathtub-shaped HR and compare it with five other popular bathtub-shaped methodologies. The results indicate that the MEW model provided the best description of the two failure time data sets, suggesting that the proposed model could be a viable candidate for solving various real-life problems.

INDEX TERMS Bathtub-shape hazard rate, exponential-Weibull model, moments, residual life, Hamiltonian Monte Carlo simulation, time to failure data.

I. INTRODUCTION

One of the most important non-monotone shapes of the hazard rate function (HRF) is the bathtub-Shaped. This kind of HR curve usually arises when it is possible to treat the population as divided into multiple sub-populations, for instance in situations where the distribution of time until failure consists of initial failures, failures due to wear and tear, and failures that occur at a relatively constant rate [1]. Hence, the ideal bathtub-shaped has two change points encompassed by a constant segment, as shown in Figure 1. The advantages of bathtub-shaped hazard rate (HR) are widely acknowledged in various fields, to mention few: [2] conducted an analysis of conditional failure rates and utilized the expected failure rate to prioritize the replacement of water pipelines. The pipes were categorized by age and type, and the expected number of breaks in the upcoming years was predicted. The maintenance schedule was determined based on the age of the pipe, with the assistance of the bathtub curve. Reference [3] examined the reliability and life prediction of power converter components. The lifespan of power electronic devices was determined by the failure rate of each individual device. The study evaluated the failure rate of power semiconductor devices by taking into account certain influential variables. The life span of the device was determined using the bathtub curve.

The associate editor coordinating the review of this manuscript and approving it for publication was Chong Leong Gan.

In addition, [4] examined the implications of using an alternative bathtub model that is based on the arcsine distribution. The author highlighted the significance of the model by presenting three case studies that focused on data sets from an engine fan, microcomputer, and crystal oscillator. The studies demonstrated the importance of the alternative bathtub model in terms of reliability analysis. Reference [5] utilized the Weibull distribution to analyze the failure rate and probability density function of a shovel-dumper system in an open cast coal mine from a reliability perspective. The authors discussed the use of the bathtub model in conjunction with the Weibull distribution to represent the failure rates of both the shovels and dumpers. Reliability Workbench is considered to analyze the failure data and demonstrated the application of the bathtub model using time between failures and time to repair data sets.

Moreover, [6] illustrated the effectiveness of the q-Weibull distribution in analyzing the reliability of computed tomography (CT) equipment failure data. The authors demonstrated that the q-Weibull distribution could effectively describe the entire bathtub curve, which is a graphical representation of the failure rate over time. The q-Weibull enabled to analyze the CT equipment failure data and gain insights into the equipment's reliability. Reference [7] examined the reliability evaluation of electronic devices using a bathtub curve derived from the extension of the exponentiated-perks distribution. Reference [8] demonstrated the practical use of the bathtub-shaped curve in reliability analysis and quality control based on the beta-Weibull distribution and the inverse power law; and has proven effective in modeling the failure times of electronic components and analyzing the quality of manufactured products. Specifically, the author studied various parameters such as the mean time to failure, and failure rate to discuss the performance of the capacitor under analysis to obtain meaningful insights. Reference [9] used the bathtub hazard rate function from the modified extension of weibull model to analyzed the failure characteristics of some aerospace electronic components. They demonstrate how the function can be used to evaluate the reliability of the components under different stress levels and to optimize the maintenance schedule to minimize downtime and cost.

A significant importance is attached to this kind of HR curve in industrial practice, essentially in burn-in strategies study to improve system reliability [10]. Yet, it has always been difficult to model data sets with obvious bathtub distributions due to the associated data complexity.

In parametric analysis, lifetime models having explicit physical interpretations pertinent to actual system or device failure times are more desirable than distributions lacking such interpretations. Recently, [11]introduced the exponential-Weibull (EW) distribution as a suitable model for analyzing the failure times of a system composed of two independent and simultaneous sub-systems operating in series. This means that the system fails when at least one of the sub-systems fails. The EW distribution has been shown to provide better fits than other classical and extended

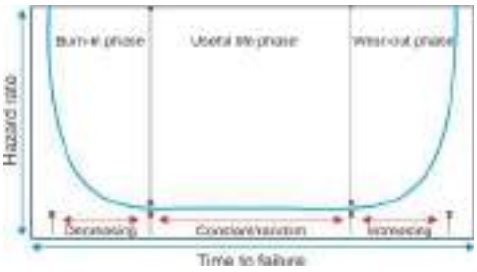

FIGURE 1. Description of bathtub-shaped hazard rate.

distributions, including the four-parameter additive Weibull (AddW) distribution [12], for data sets characterized by monotone HRs. The EW distribution has a clear physical interpretation and was specifically designed to accommodate failure times arising from a series system with two sub-systems functioning independently. The time to failure of the system is defined by the random variable $T = \min\{Y, Z\}$, where Y and Z are the failure times of the first and second sub-systems, respectively. Y is assumed to have an exponential distribution, while Z has a Weibull distribution. A random variable T is said to have a two-parameter EW distribution if its cumulative distribution function (CDF) is given by:

$$F(t) = 1 - \exp\left(-\lambda t - t^{\alpha}\right), \quad t > 0,\ \alpha, \lambda > 0. \qquad (1)$$

where α, and λ are the distribution parameters. However, it is important to note that the two-parameter EW distribution is not suitable for modeling data sets with non-monotone hazard rates, as demonstrated by [13]. The HRF of the distribution is increasing when the only shape parameter $\alpha < 1$ and is decreasing if $\alpha > 1$. That is, the underlying distribution of Y and Z from the two sub-system need to have monotone HRs. However, often in reliability studies, quality control analysis and survival analysis, lifetime data sets possess non-monotone HRs and therefore the use of EW model in the study and prediction of failure of a system or individual survival time may not provide the approximate description of the actual situation. The bathtub-shaped and unimodal are the frequently encountered HRs among other non-monotone HRs. Where the bathtub-shaped HRF remains the most important shape every model struggle to possess (see [14], [15] for details on different forms of bathtub HRF). Considering the limited flexibility of EW distribution, several works were carried out to modified the model. The transmuted exponential-Weibull (TEW), Kumaraswamy exponential-Weibull (KwEW), Gamma exponentiated exponential-Weibull (GEEW) and generalized extended exponential-Weibull (GExtEW) are recently introduced by Saboor et al. [16], Cordeiro et al. [17], Pogány and Saboor [18], and Shakhatreh et al. [13].

Although, the TEW, KwEw, GEEW, and GExtEW extended the EW distribution by adding parameter(s) through different modification methods, the distributions are found to be better in practice than the EW distribution. The TEW, KwEW, GEEW, and GExtEW distributions are learned to

have exhibited at least one non-monotone HR shape, and notwithstanding, can not adequately describe lifetime data that have one or two failure modes with clear bathtub-shaped HR such as the cable joint failure data sets reported by Tang et al. [19] and Tang et al. [20], and the well-known device failure times data set by Meeker et al. [21]. This drawback may happen since their modifications does not take into account the physical interpretation of the EW distribution.

On the other hand, several extension of Weibull distribution with similar physical interpretation to EW distribution are defined. These include the new modified Weibull [22], additive modified Weibull [23], Weibull Lindley [24], log-normal modified Weibull [15], improved new modified Weibull [25], Weibull-Chen [26], additive Chen Weibull [27], flexible additive Chen-Gompertz [28], and additive Gompertz-Weibull [29] distributions.

In view of the deficiencies identified with EW distribution and its extensions and with no study that extended the distribution while reserving its practical interpretation, we propose to extend the EW distribution to allow the random variable $T = \min\{Z, Y\}$ accommodate monotone and non-monotone HR distributions. In this case, either the distribution of Z or Y can have monotone or non-monotone HR function. The modified EW (abbreviated as MEW) distribution, is constructed by replacing T in Eq.(1) with

$$G(t)/\bar{G}(t), \quad and \quad [\bar{G}(t) = 1 - G(t)],$$

where $G(t) = 1-\exp((t/\theta)^{\gamma})$ is the CDF of standard Weibull distribution. Hence, we have the CDF of the modified model as given in Eq.(2). One interesting flexibility of the MEW model over the other extensions of EW distributions is that it can accommodate $T = \min\{Z, Y\}$ with both Z and Y having non-monotone HR function. This is contrary to many additive models, where either both the HR of Z and Y are monotone (such as in EW and AddW distributions) or only one of the baseline random variables has non-monotone HR (like the case of AMW, NMW, and ACW models). The advantages of the adopted modification procedure has been recognized in different notable studies, such as [30] and [31].

The enhanced distribution has greater flexibility, due to the transformation and added shape parameter. It has depicted several types of HR shapes, including the notable bathtub curve labeled in FIGURE 1 and can be adopted in modeling different failure time data sets. We present Bayesian technique and maximum likelihood procedure for estimating the four unknown model parameters. Contrary to many studies verifying their distributions' applicability using complete/uncensored data, here, we demonstrate the potential of the MEW model using censored and uncensored failure time data sets. The enhanced distribution best fits the considered data sets in comparisons with other recent models based on some known model selection criteria and plots.

After justifying the study purpose and problem to be addressed, and how to define a flexible distribution with bathtub-shaped HR function in Section I, we then proceed to describe the modified model in Section II, including the model interpretation as well as some shapes of density and HR functions. Section III presents some properties of the distribution. In Sections IV, we provide information on how to use both the maximum likelihood and Bayesian approach to estimate the parameters of the distribution. In Section V, we demonstrate the practical applications of the distribution using real-world data. Lastly, in Section VI, we summarize and conclude the paper.

II. THE MEW DISTRIBUTION

Here, to modify the EW model, first we consider the model transformation by odd function and transform the random variable T in Eq.(1). The odds function of the CDF of standard Weibull model is defined by as $G(t)/(1 - G(t)) = \exp((t/\theta)^{\gamma})-1$. Thus, the CDF of the proposed MEW having four-parameter vector $\boldsymbol{\varphi} = (\alpha, \gamma, \theta, \lambda)'$ is given by

$$F(t) = 1 - \exp\left\{\lambda(1 - e^{(t/\theta)^{\gamma}}) - (e^{(t/\theta)^{\gamma}} - 1)^{\alpha}\right\}, \quad t > 0, \tag{2}$$

where $\alpha > 0$, and $\gamma \geq 0$ are MEW's shape parameters, and $\lambda \geq 0$ and $\theta > 0$ represents the model's scale parameters. The model was intended to have two shape and two scale parameters that is why the two parameter EW in Eq.(1) is considered, and it helps in getting reliable optimization results in estimation process. Eq.(2) can be viewed in two different ways. The first as an extension of EW distribution. While the second as an additive model with modified Weibull extension (MWE) [32] and three-parameter improved Weibull-Weibull (IWW3) [33] distributions as the hybrid baseline models. That is, Eq.(2) can be written as $F(t) = 1-S_{MWE}(t)S_{IWW3}(t)$, where $S_{MWE}(t)$ and $S_{IWW3}(t)$ are the survival functions of the MWE and IWW3 distributions, respectively.

The associated probability density function (PDF) is given by

$$f(t) = \frac{\gamma\left[\lambda + \alpha(e^{(t/\theta)^{\gamma}} - 1)^{\alpha-1}\right]}{\theta(t/\theta)^{-\gamma+1}e^{-(t/\theta)^{\gamma}}} \times \exp\left\{\lambda(1 - e^{(t/\theta)^{\gamma}}) - (e^{(t/\theta)^{\gamma}} - 1)^{\alpha}\right\}, \quad t > 0. \tag{3}$$

FIGURE 2 presents the PDF curves of the MWE distribution.

It can be noted that the shape of the density function varies depending on the parameter values, with some examples in FIGURE 2 including decreasing, unimodal, and modified bathtub shapes characterized by a pattern of decreasing-increasing-decreasing. The reliability/survival function and hazard rate function are expressed separately, with the (SF) representing reliability/survival and the (HRF) representing the hazards rate function.

$$S(t) = \exp\left\{\lambda(1 - e^{(t/\theta)^{\gamma}}) - (e^{(t/\theta)^{\gamma}} - 1)^{\alpha}\right\}, \quad t > 0, \tag{4}$$

and

$$h(x) = \frac{\gamma\left[\lambda + \alpha(e^{(t/\theta)^{\gamma}} - 1)^{\alpha-1}\right]}{\theta(t/\theta)^{-\gamma+1}e^{-(t/\theta)^{\gamma}}}, \quad t > 0. \tag{5}$$

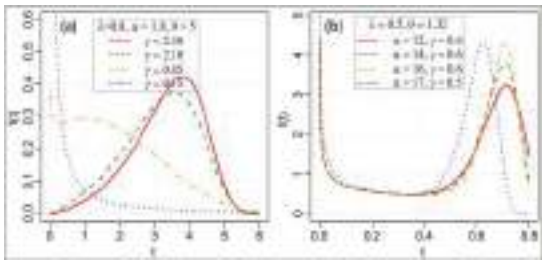

FIGURE 2. Various MEW density function curves under different settings of the parameter values.

Glaser [34] discuss the adequate conditions to characterize a given distribution with non-monotone HR. The HRF of the MEW model, which depends on the two shape parameters $\gamma > 0$ and $\alpha > 0$, presents bathtub-shaped when $h'(t^*) = 0$ if and only if $t = t^*$ is the root of the equation:

$$[(\gamma-1)t^{*-1}+\gamma\theta^{-\gamma}t^{*\gamma-1}]h(t^*)+(\alpha-1)t^{*\gamma-1}(1-e^{-(t^*/\theta)^\gamma})^{-1}=0,$$

where $h'(t) = \frac{\mathrm{d}h(t)}{\mathrm{d}t}$ is the derivative of the HRF in (5). It is verifiable that the HRF is decreasing if $h'(t) < 0$ for $t < t^*$ and is increasing if $h'(t) > 0$ for $t > t^*$. The figure 3(a)-(c) displays the HRF plots for different parameter values in the improved model, which incorporates multiple HRF shapes to describe intricate failure time data. In particular, figure 3(c) illustrates the bathtub-shaped HR curve that includes a long-flat segment (known as the useful lifetime). The usefulness of a bathtub-shaped HR with a long or long-flat useful lifetime is significant for reliability and other survival time analysis. It is interesting that the HRF of MEW possessed this quality; as a result, MEW can be extremely useful in this context. The MEW distribution has an advantage over the other EW model extensions because it is the only EW extension that preserves the EW physical interpretation while also presenting this type of bathtub-shaped HR curve.

III. DISTRIBUTION PROPERTIES

In this section we derive and discuss various properties of the MEW model.

A. QUANTILES, MEDIAN AND MODE

Quantile function is an indispensable function in statistical studies in both theoretical and applied studies such as generating random data, model estimation, extreme values studies, graphical analysis, mean residual analysis, etc. (see, [35], [36], [37]). The quantile t_q, for $0 < q < 1$ of the MEW model can be gotten by the real solution of the given nonlinear equation

$$\lambda e^{(t/\theta)^\gamma} + (e^{(t/\theta)^\gamma} - 1)^\alpha = \lambda - \log(1-q). \qquad (6)$$

Eq.(6) does not have a closed-form solution in t_q, and thus, we adopt a numerical solution technique to determine the quantile. Following we presents a simple algorithm for deriving random samples from the MEW($\gamma, \alpha, \theta, \lambda$).

Step 1 Generate $q_i \sim U(0,1)$, $i = 1, 2, \ldots, n$, and then
Step 2 apply **Step 1** to calculate for t_{qi} in

$$\lambda e^{(t_{qi}/\theta)^\gamma} + (e^{(t_{qi}/\theta)^\gamma} - 1)^\alpha = \lambda - \log(1-q_i).$$

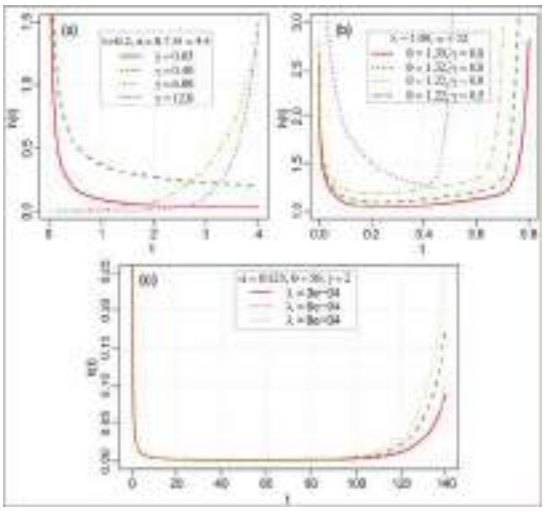

FIGURE 3. MEW hazard rate function curves: (a) increasing and decreasing shapes, (b) bathtub-shaped without long-flat segment, and (c) bathtub-shaped with long-flat phase for different parameter settings.

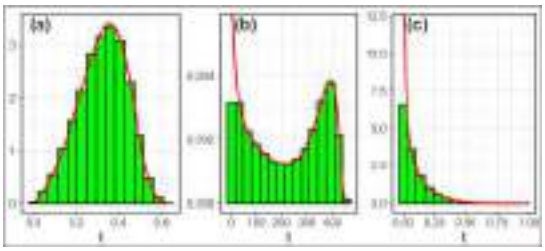

FIGURE 4. Histograms and MEW density curves of three simulated samples each with $n = 10000$: (a) $\alpha = 1.5, \gamma = 2.0, \lambda = 0.5, \theta = 0.5$, (b) $\alpha = 0.1, \gamma = 7.0, \lambda = 0.7, \theta = 400$, and (c) $\alpha = 0.5, \gamma = 0.8, \lambda = 2.0, \theta = 0$.

To investigate the consistency of the generated samples from Eq.(6), we display the histograms and MEW density curves of the simulated samples in FIGURE 4(a)-(c). From FIGURE 4, we observe that the generated samples are consistent. Eq.(6) gives the median of the MEW random variable T at $q = 1/2$.

The mode of the MEW distribution is the value of T at which the density function $f(t) = h(t)S(t)$ reaches its highest point. Therefore, the Eq. (7) can be solved to find the value of T that corresponds to the mode.

$$h'(t)S(t) + h(t)S'(t) = 0, \qquad (7)$$

where $h'(t)$ and $S'(t)$ are respectively obtained as the derivatives of HRF and SF functions,

$$h'(t) = \left[(\gamma-1)t^{-1} + \gamma\theta^{-\gamma}t^{\gamma-1}\right]h(t) + (\alpha-1)t^{\gamma-1}(1-e^{-(t/\theta)^\gamma})^{-1},$$
$$S'(t) = -\gamma\theta^{-\gamma}t^{\gamma-1}e^{(t/\theta)^\gamma}(\lambda + \alpha(e^{(t/\theta)^\gamma} - 1)^{\alpha-1})S(t).$$

Eq.(7) lacks a practical analytical expression, hence it necessitates the use of numerical techniques.

B. RELIABILITY

Mean residual life (MRL) and Mean time to failure (MTTF) are important tools in reliability analysis and can help

predict the expected lifetime and failure rate of a system or component.

1) MEAN RESIDUAL LIFE

MRL represents the period from a specific time x to the failure time of an individual or system. That is, it determine the expected remaining lifetime of a component, system or individual with age x at present. Residual life are also used to characterized distribution uniquely (see, [38]). In [39], the author explores the connections between the MRL and HRF, with a particular focus on bathtub-shaped models. Four extensions of the Weibull are analyzed, specifically in regards to their change points and the variations between them. The article also delves into additional concerns surrounding the flatness of the bathtub curve. We refer to [40] for more applications of MRL in reliability engineering, quality control, risk management, life testing, and maintenance optimization. The MRL of the MEW is computed as:

$$\begin{aligned}\mu_T(x) &= E(T-x|T>x)\\ &= \frac{1}{S(x)}\int_x^{+\infty} S(t)\,\mathrm{d}t = \frac{1}{S(x)}\int_0^{+\infty} S(t+x)\,\mathrm{d}t\\ &= \frac{e^{\lambda}}{S(x)}\sum_{i,j=0}^{+\infty}\sum_{p=0}^{+\infty}\upsilon_{i,j}\upsilon_p\int_0^{+\infty}(t+x)^{j\gamma}e^{-p\theta^{-\gamma}(t+x)^{\gamma}}\,\mathrm{d}t\\ &= \frac{e^{\lambda e^{(x/\theta)^{\gamma}}+\left(e^{(x/\theta)^{\gamma}}-1\right)^{\alpha}}}{\gamma}\\ &\quad\times\sum_{i,j=0}^{+\infty}\sum_{p=0}^{+\infty}\upsilon_{i,j}\upsilon_p\frac{\theta^{j\gamma+1}}{p^{(j\gamma+1)/\gamma}}\gamma\left(\frac{j\gamma+1}{\gamma}\right), \qquad (8)\end{aligned}$$

where $\upsilon_{i,j} = (-\lambda)^i(i)^j/i!j!\theta^{j\gamma}$, $\upsilon_p = \sum_{k,\ell=0}^{+\infty}(-1)^p\gamma(k\alpha+\ell+1)\upsilon_{k,\ell}/p!\gamma(k\alpha+\ell-p+1)$ and $\upsilon_{k,\ell} = (-1)^k\gamma(k\alpha+\ell)/k!\ell!\gamma(k\alpha)$, and $\gamma(.)$ is the gamma function.

2) MEAN TIME TO FAILURE

MTTF is the average time until the variable fails or stops working. It represents the expected value of the time to failure. We define the MEW model MTTF as:

$$\begin{aligned}MTTF &= \int_0^{+\infty} S(t)\,\mathrm{d}t\\ &= \int_0^{+\infty} e^{\lambda\left(1-e^{(t/\theta)^{\gamma}}\right)-\left(e^{(t/\theta)^{\gamma}}-1\right)^{\alpha}}\,\mathrm{d}t\\ &= e^{\lambda}\sum_{i,j=0}^{+\infty}\sum_{p=0}^{+\infty}\upsilon_{i,j}\upsilon_p\int_0^{+\infty}t^{j\gamma}e^{-p(t/\theta)^{\gamma}}\,\mathrm{d}t\\ &= \frac{e^{\lambda}}{\gamma}\sum_{i,j=0}^{+\infty}\sum_{p=0}^{+\infty}\upsilon_{i,j}\upsilon_p\frac{\theta^{j\gamma+1}}{p^{(j\gamma+1)/\gamma}}\gamma\left(\frac{j\gamma+1}{\gamma}\right),\end{aligned}$$

where $\upsilon_{i,j}$, $\upsilon_{k,\ell}$ and υ_p are given in Eq.(8), and $\gamma(.)$ is the gamma function.

To explore the characteristics of MRL ($\mu_T(x)$) and MTTF of MEW distribution at varying parameter values, we provide some Monte Carlo simulation and numerical integration values along with their respective errors in TABLEs 1-2. The simulation outputs were derived from $N = 1000$ random samples based on the sizes 50, 100, 200 and 300, respectively, under two parameter settings. Four time points $x = 0.01, 0.2, 0.6$, and 0.8 were taken for the $\mu_T(x)$. It is learned that the $\mu_T(x)$ and MTTF are tend to the same value as x decreases to 0, that is, MRL of a device or individual converges to the MTTF as $x \to 0$. The findings depict a fall in the $\mu_T(x)$ estimates under both Monte Carlo and numerical integration methods as x increases over a fixed sample size n. A consistent decrease in standard deviations (between parenthesis) for the Monte Carlo results is observed. It can be seen that the two methods produce more comparable values when the shape parameter α is above unity.

C. MOMENTS

Moments are critical tools in statistical studies and can be used to describe several distribution characteristics. For $T \sim$ MEW$(\alpha, \gamma, \lambda, \theta)$, the computation of the r^{th} non-central moments is achievable in the following way: considering the Taylor series of e^t, then Binomial expansion of $(1+t)^{b-1}$, for b real and non-integer, also, $|t| < 1$.

$$\begin{aligned}\mu_r &= \int_0^{+\infty} t^r\,\mathrm{d}F(t)\\ &= \int_0^{+\infty} rt^{r-1}e^{\lambda\left(1-e^{(t/\theta)^{\gamma}}\right)-\left(e^{(t/\theta)^{\gamma}}-1\right)^{\alpha}}\,\mathrm{d}t\\ &= re^{\lambda}\sum_{i,j=0}^{+\infty}\sum_{p=0}^{+\infty}\upsilon_{i,j}\upsilon_p\int_0^{+\infty}t^{j\gamma+r-1}e^{-p(t/\theta)^{\gamma}}\,\mathrm{d}t\\ &= \frac{re^{\lambda}}{\gamma}\sum_{i,j=0}^{+\infty}\sum_{p=0}^{+\infty}\upsilon_{i,j}\upsilon_p\frac{\theta^{j\gamma+r}}{p^{(j\gamma+r)/\gamma}}\gamma\left(\frac{j\gamma+r}{\gamma}\right),\\ &\quad for \quad r=1,2,\ldots,\end{aligned}$$

where $\upsilon_{i,j}$, $\upsilon_{k,\ell}$ and υ_p are given in Eq.(8), and $\gamma(.)$ a gamma function. Direct usage of Eq.(8) may be difficult; however, numerical integration and Monte Carlo simulation could alternatively be applied for computing different distributional properties of MEW from the moments, such as the variance (σ^2), skewness ($\sqrt{\beta_1}$) and kurtosis (β_2).

TABLEs 5-6 report the Monte Carlo simulation results for the first four non-central moments (μ_1', μ_2', μ_3', and μ_4'), variance (σ^2), skewness ($\sqrt{\beta_1}$) and kurtosis (β_2) with their respective standard deviations (SDs) between parenthesis. The estimates of the properties were computed for nine distinct combinations of MEW parameters, and random samples $N = 1000$ base on sizes $n = 50, 100, 200$ and 300. For each parameter setting, the estimates are seen to be closed to each other with decrease in SDs over different sample sizes. All the seven computed characteristics of the distribution deceases when γ is less than unity over an increase in α. Contrarily, the kurtosis β_2 rises when $\gamma > 1$ and over the increase in α.

TABLE 1. Results for MRL ($\mu_T(x)$) and MTTF using Monte Carlo simulation and numerical integration with standard deviation and integration error reported between parentheses; $\alpha = 0.3, \gamma = 2.5, \lambda = 0.2, \theta = 1.2$.

$n\downarrow$		MRL		MTTF	
	$t\downarrow$	Monte Carlo	Numerical integration	Monte Carlo	Numerical integration
	0.01				
50		0.6941 (0.0729)	0.7134 (3.74×10^{-5})	0.7040 (0.0727)	0.7038 (9.67×10^{-5})
100		0.6940 (0.0515)		0.7042 (0.0523)	
200		0.6942 (0.0363)		0.7058 (0.0364)	
300		0.6923 (0.0307)		0.7034 (0.0302)	
	0.2				
50		0.4893 (0.0910)	0.6884 (1.99×10^{-5})	-	-
100		0.4959 (0.0574)		-	-
200		0.4943 (0.0421)		-	-
300		0.4949 (0.0343)		-	-
	0.4				
50		0.2949 (0.0954)	0.6134 (5.88×10^{-5})	-	-
100		0.2941 (0.0635)		-	-
200		0.2953 (0.0472)		-	-
300		0.2934 (0.0384)		-	-
	0.6				
50		0.0930 (0.0946)	0.5242 (1.88×10^{-6})	-	-
100		0.0898 (0.0755)		-	-
200		0.0935 (0.0542)		-	-
300		0.0946 (0.0411)		-	-
	0.8				
50		0.0046 (0.0084)	0.4289 (4.24×10^{-6})	-	-
100		0.0033 (0.0078)		-	-
200		0.0064 (0.0061)		-	-
300		0.0050 (0.0053)		-	-

TABLE 2. Results for MRL ($\mu_T(x)$) and MTTF using Monte Carlo simulation and numerical integration with standard deviation and integration error reported between parentheses; $\alpha = 1.2, \gamma = 2.5, \lambda = 0.2, \theta = 1.2$.

$n\downarrow$		MRL		MTTF	
	$t\downarrow$	Monte Carlo	Numerical integration	Monte Carlo	Numerical integration
	0.01				
50		0.8660 (0.0374)	0.8654 (2.50×10^{-6})	0.8748 (0.0377)	0.8754 (1.27×10^{-6})
100		0.8662 (0.0276)		0.8758 (0.0268)	
200		0.8660 (0.0192)		0.8750 (0.0190)	
300		0.86573 (0.0151)		0.8755 (0.0146)	
	0.2				
50		0.6667 (0.0379)	0.6712 (1.48×10^{-6})	-	-
100		0.6659 (0.0258)		-	-
200		0.6654 (0.0183)		-	-
300		0.6652 (0.0155)		-	-
	0.4				
50		0.4642 (0.0382)	0.4981 (6.37×10^{-6})	-	-
100		0.4646 (0.0279)		-	-
200		0.4654 (0.0193)		-	-
300		0.4656 (0.0162)		-	-
	0.6				
50		0.2642 (0.0404)	0.3525 (2.90×10^{-6})	-	-
100		0.2658 (0.0290)		-	-
200		0.2645 (0.0207)		-	-
300		0.2658 (0.0172)		-	-
	0.8				
50		0.0658 (0.0469)	0.2352 (3.19×10^{-6})	-	-
100		0.0641 (0.0335)		-	-
200		0.0657 (0.0248)		-	-
300		0.0645 (0.0207)		-	-

IV. ESTIMATION

Within this section, we will examine the process of determining the MEW unknown parameters using both maximum likelihood estimation (MLE) and Bayesian estimation methods.

A. MLE FOR NON-CENSORED DATA

Maximum likelihood technique is the commonly used statistical inference method. This method is reliable and offers advantages in theoretical studies and asymptotic efficiency, there is an extensive literature regarding this method (see, [41] and [42]). Suppose we have a random sample of size n, denoted by $t_1, t_2, \ldots, t_n$, from the MEW model

TABLE 3. First four moments, variance, skewness and kurtosis 1000 simulated samples of sizes $n = 50$ and 100; standard deviations between parentheses.

	$n=50$			$n=100$		
$\gamma\rightarrow$	0.9	1.5	2.5	0.9	1.5	2.5
	$\alpha=0.3,\lambda=0.2,\theta=1.2$					
μ_1'	0.6435 (0.1233)	0.6365 (0.0900)	0.6990 (0.0727)	0.6551 (0.0838)	0.6453 (0.0613)	0.7059 (0.0502)
μ_2'	1.1726 (1.1624)	0.8121 (0.8121)	0.7538 (0.1894)	1.2006 (0.7897)	0.8281 (0.2423)	0.7654 (0.1288)
μ_3'	2.7669 (0.3561)	1.2597 (0.1743)	0.9429 (0.1187)	2.8426 (0.2435)	1.2887 (0.1187)	0.9606 (0.0807)
μ_4'	7.5160 (4.1331)	2.1658 (0.7560)	1.2753 (0.3079)	7.7392 (2.7787)	2.2208 (0.5161)	1.3023 (0.2101)
σ^2	0.7586 (0.2172)	0.4071 (0.0773)	0.2653 (0.0376)	0.7722 (0.1474)	0.4120 (0.0521)	0.2673 (0.0250)
$\sqrt{\beta_1}$	1.5045 (0.3707)	0.8464 (0.2622)	0.3230 (0.2206)	1.5156 (0.2595)	0.8355 (0.1733)	0.3092 (0.1473)
β_2	4.6033 (1.6344)	2.6621 (0.6473)	1.9309 (0.2651)	4.6636 (1.1766)	2.6182 (0.4197)	1.8898 (0.1611)
	$\alpha=0.6,\lambda=0.2,\theta=1.2$					
μ_1'	0.6110 (0.0922)	0.6864 (0.0703)	0.7938 (0.0552)	0.6199 (0.0630)	0.6931 (0.0486)	0.7988 (0.0388)
μ_2'	0.7990 (0.5645)	0.7206 (0.2245)	0.7845 (0.1397)	0.8165 (0.3814)	0.7323 (0.1528)	0.7934 (0.0954)
μ_3'	1.3969 (0.2156)	0.9151 (0.1256)	0.8714 (0.0922)	1.4336 (0.1467)	0.9341 (0.0856)	0.8847 (0.0634)
μ_4'	2.8945 (1.6324)	1.3037 (0.4186)	1.0433 (0.2111)	2.9778 (1.0895)	1.3348 (0.2843)	1.0624 (0.1438)
σ^2	0.4256 (0.1200)	0.2495 (0.0471)	0.1544 (0.0249)	0.4326 (0.0810)	0.2521 (0.0317)	0.1554 (0.0170)
$\sqrt{\beta_1}$	1.3003 (0.3636)	0.5941 (0.2456)	0.0515 (0.2167)	1.3343 (0.2620)	0.5964 (0.1660)	0.0421 (0.1447)
β_2	4.2562 (1.5653)	2.5600 (0.5561)	2.1729 (0.2673)	4.4294 (1.2061)	2.5601 (0.3765)	2.1560 (0.1699)
	$\alpha=1.2,\lambda=0.2,\theta=1.2$					
μ_1'	0.6056 (0.0598)	0.7434 (0.0484)	0.8732 (0.0372)	0.6113 (0.0414)	0.7478 (0.0340)	0.8763 (0.0264)
μ_2'	0.5472 (0.1645)	0.6713 (0.1112)	0.8327 (0.0888)	0.5562 (0.1115)	0.6787 (0.0759)	0.8385 (0.0613)
μ_3'	0.6093 (0.0984)	0.6812 (0.0771)	0.8435 (0.0629)	0.6222 (0.0670)	0.6915 (0.0531)	0.8519 (0.0439)
μ_4'	0.7782 (0.2933)	0.7497 (0.1607)	0.8936 (0.1198)	0.7974 (0.1972)	0.7636 (0.1092)	0.9050 (0.0821)
σ^2	0.1805 (0.0393)	0.1187 (0.0211)	0.0702 (0.0133)	0.1826 (0.0265)	0.1196 (0.0144)	0.0706 (0.0094)
$\sqrt{\beta_1}$	0.7125 (0.2900)	0.1253 (0.2374)	-0.3204 (0.2568)	0.7314 (0.2027)	0.1219 (0.1588)	-0.3405 (0.1716)
β_2	2.9820 (0.8537)	2.3890 (0.3601)	2.6134 (0.4525)	3.0479 (0.6304)	2.3874 (0.2378)	2.6281 (0.3099)

TABLE 4. First four moments, variance, skewness and kurtosis for 1000 simulated samples of sizes $n = 200$ and 300; standard deviations between parentheses.

	$n=200$			$n=300$		
$\gamma\rightarrow$	0.9	1.5	2.5	0.9	1.5	2.5
	$\alpha=0.3,\lambda=0.2,\theta=1.2$					
μ_1'	0.6533 (0.0631)	0.6436 (0.0460)	0.7044 (0.0370)	0.6491 (0.0501)	0.6408 (0.0369)	0.7023 (0.0300)
μ_2'	1.1973 (0.5941)	0.8258 (0.1810)	0.7634 (0.0969)	1.1873 (0.4592)	0.8199 (0.1413)	0.7595 (0.0768)
μ_3'	2.8322 (0.1818)	1.2851 (0.0891)	0.9579 (0.0607)	2.8137 (0.1414)	1.2745 (0.0704)	0.9515 (0.0486)
μ_4'	7.6983 (2.1156)	2.2142 (0.3861)	1.2987 (0.1573)	7.6856 (1.6521)	2.1964 (0.2989)	1.2886 (0.1237)
σ^2	0.7704 (0.1090)	0.4115 (0.0381)	0.2671 (0.0182)	0.7660 (0.0850)	0.4093 (0.0298)	0.2662 (0.0142)
$\sqrt{\beta_1}$	1.5268 (0.1899)	0.8437 (0.1321)	0.3153 (0.1115)	1.5558 (0.1661)	0.8555 (0.1100)	0.3204 (0.0897)
β_2	4.6831 (0.8444)	2.6190 (0.3093)	1.8840 (0.1226)	4.8271 (0.7614)	2.6544 (0.2696)	1.8905 (0.1037)
	$\alpha=0.6,\lambda=0.2,\theta=1.2$					
μ_1'	0.6183 (0.0472)	0.6917 (0.0359)	0.7977 (0.0281)	0.6154 (0.0376)	0.6896 (0.0291)	0.7962 (0.0231)
μ_2'	0.8140 (0.2889)	0.7304 (0.1148)	0.7917 (0.0715)	0.8085 (0.2241)	0.7265 (0.0896)	0.7889 (0.0568)
μ_3'	1.4278 (0.1103)	0.9313 (0.0643)	0.8825 (0.0471)	1.4210 (0.0858)	0.9251 (0.0509)	0.8780 (0.0380)
μ_4'	2.9612 (0.8350)	1.3304 (0.2141)	1.0595 (0.1080)	2.9651 (0.6601)	1.3218 (0.1658)	1.0531 (0.0850)
σ^2	0.4316 (0.0603)	0.2519 (0.0232)	0.1554 (0.0121)	0.4298 (0.0467)	0.2509 (0.0179)	0.1550 (0.0095)
$\sqrt{\beta_1}$	1.3520 (0.1943)	0.6051 (0.1249)	0.0458 (0.1075)	1.3848 (0.1723)	0.6170 (0.1042)	0.0508 (0.0860)
β_2	4.4873 (0.8983)	2.5654 (0.2784)	2.1509 (0.1231)	4.6615 (0.8312)	2.6037 (0.2486)	2.1575 (0.1054)
	$\alpha=1.2,\lambda=0.2,\theta=1.2$					
μ_1'	0.6102 (0.0305)	0.7468 (0.0246)	0.8756 (0.0189)	0.6084 (0.0247)	0.7455 (0.0203)	0.8746 (0.0157)
μ_2'	0.5547 (0.0842)	0.6773 (0.0569)	0.8373 (0.0453)	0.5519 (0.0655)	0.6750 (0.0450)	0.8355 (0.0366)
μ_3'	0.6202 (0.0504)	0.6898 (0.0394)	0.8503 (0.0320)	0.6168 (0.0397)	0.6865 (0.0317)	0.8476 (0.0262)
μ_4'	0.7943 (0.1502)	0.7614 (0.0822)	0.9030 (0.0613)	0.7914 (0.1171)	0.7572 (0.0643)	0.8993 (0.0490)
σ^2	0.1824 (0.0196)	0.1195 (0.0103)	0.0706 (0.0065)	0.1818 (0.0150)	0.1192 (0.0081)	0.0705 (0.0053)
$\sqrt{\beta_1}$	0.7436 (0.1515)	0.1259 (0.1183)	-0.3444 (0.1261)	0.7631 (0.1307)	0.1337 (0.0960)	-0.3414 (0.0992)
β_2	3.0712 (0.4705)	2.3871 (0.1721)	2.6369 (0.2189)	3.1525 (0.4371)	2.4050 (0.1546)	2.6406 (0.1749)

with parameter vector $\varphi = (\alpha, \gamma, \lambda, \theta)'$. The log-likelihood function of φ can be obtained from the PDF in (3) as

$$\ell(\varphi) = n\log\gamma - n\gamma\log\theta + (\gamma-1)\sum_{i=1}^{n}\log t_i + \sum_{i=1}^{n}(t_i/\theta)^{\gamma} + \sum_{i=1}^{n}\log(c_i) - \sum_{i=1}^{n}\left(\lambda a_i + a_i^{\alpha}\right), \quad (9)$$

where $a_i = e^{(t_i/\theta)^{\gamma}} - 1$, and $c_i = \lambda + \alpha a_i^{\alpha-1}$. Let $\widehat{\varphi}$ be the estimates, the determination of $\widehat{\varphi}$ can be achieved through the maximization of (9) or by solving its derivative with respect to each parameter. Thus, we arrived at the following score functions.

$$\frac{\partial\ell}{\partial\lambda} = \sum_{i=1}^{n}\frac{1}{c_i} - \sum_{i=1}^{n}a_i,$$

$$\frac{\partial\ell}{\partial\alpha} = \sum_{i=1}^{n}\frac{a_i^{\alpha-1}}{c_i}(1+\alpha\log(a_i)) - \sum_{i=1}^{n}a_i^{\alpha}\log(a_i),,$$

$$\frac{\partial\ell}{\partial\theta} = -\frac{n\gamma}{\theta} - \frac{\gamma}{\theta}\sum_{i=1}^{n}(t_i/\theta)^{\gamma} + \frac{\gamma\alpha(\alpha-1)}{\theta}\sum_{i=1}^{n}\frac{a_i^{\alpha}b_i}{a_i^2c_i}$$

$$+\frac{\gamma}{\theta}\sum_{i=1}^{n}\frac{b_i}{c_i}$$

$$\frac{\partial \ell}{\partial \gamma}=\frac{n}{\gamma}-n\log\theta+\sum_{i=1}^{n}\log t_i+\alpha(\alpha-1)\sum_{i=1}^{n}\frac{a_i^{\alpha}b_i}{a_i^2c_i}\log(t_i/\theta)+\sum_{i=1}^{n}(t_i/\theta)^{\gamma}\log(t_i/\theta)-\sum_{i=1}^{n}b_ic_i\log(t_i/\theta),$$

where $a_i = e^{(t_i/\theta)^{\gamma}} - 1$, $b_i = (t_i/\theta)^{\gamma}e^{(t_i/\theta)^{\gamma}}$, and $c_i = \lambda + \alpha a_i^{\alpha-1}$. Finding solutions to these problems using analytical methods may be too difficult. As a result, a numerical technique is employed to calculate the maximum likelihood estimates (MLEs) of the unknown parameters $\varphi = (\alpha, \gamma, \lambda, \theta)'$, starting with a well-chosen set of initial values. We used the `maxLik` function from the maxLik package [43] in the `R4.2.2` software for optimization.

Additionally, we can determine the MLEs of $S(t)$ and $h(t)$ by applying the invariant property of the MLE [44]. Therefore, the MLEs of $S(t)$ and $h(t)$ are, respectively, given by

$$\hat{R}(t) = e^{\hat{\lambda}(1-e^{(t/\hat{\theta})^{\hat{\gamma}}})-(e^{(t/\hat{\theta})^{\hat{\gamma}}}-1)^{\hat{\alpha}}};$$
$$\hat{h}(t) = \hat{\gamma}\hat{\theta}^{-\hat{\gamma}}t^{\hat{\gamma}-1}e^{(t/\hat{\theta})^{\hat{\gamma}}}\left(\hat{\lambda}+\hat{\alpha}(e^{(t/\hat{\theta})^{\hat{\gamma}}}-1)^{\hat{\alpha}-1}\right).$$

1) ASYMPTOTIC CONFIDENCE INTERVALS

It is possible to determine the precise distributions of the Maximum Likelihood Estimators (MLEs), but obtaining closed-form solutions is quite challenging. Therefore, we opt to calculate an estimated confidence interval for the parameters. We base our calculation on the asymptotic normality distributions for γ, α, θ, and λ, as the sample size approaches infinity. Specifically, $\sqrt{n}\left(\varphi - \hat{\varphi}\right) \sim N_4\left(0, I^{-1}\right)$, where

$$I(\varphi) = -\begin{bmatrix} \frac{\partial^2\ell(\varphi)}{\partial\gamma^2} & \frac{\partial^2\ell(\varphi)}{\partial\gamma\partial\alpha} & \frac{\partial^2\ell(\varphi)}{\partial\gamma\partial\theta} & \frac{\partial^2\ell(\varphi)}{\partial\gamma\partial\lambda} \\ \cdot & \frac{\partial^2\ell(\varphi)}{\partial\alpha^2} & \frac{\partial^2\ell(\varphi)}{\partial\alpha\partial\theta} & \frac{\partial^2\ell(\varphi)}{\partial\alpha\partial\lambda} \\ \cdot & \cdot & \frac{\partial^2\ell(\varphi)}{\partial\theta^2} & \frac{\partial^2\ell(\varphi)}{\partial\theta\partial\lambda} \\ \cdot & \cdot & \cdot & \frac{\partial^2\ell(\varphi)}{\partial\lambda^2} \end{bmatrix}.$$

The elements of $I(\varphi)$ are given in the Appendix. Then we can have the approximate variance-covariance matrix evaluated at $\hat{\varphi} = (\hat{\gamma}, \hat{\alpha}, \hat{\theta}, \hat{\lambda})'$, the MLE of $(\gamma, \alpha, \theta, \lambda)'$ as

$$I^{-1}\left(\hat{\varphi}\right) = \begin{bmatrix} var(\hat{\gamma}) & cov(\hat{\gamma},\hat{\alpha}) & cov(\hat{\gamma},\hat{\theta}) & cov(\hat{\gamma},\hat{\lambda}) \\ \cdot & var(\hat{\alpha}) & cov(\hat{\alpha},\hat{\theta}) & cov(\hat{\alpha},\hat{\lambda}) \\ \cdot & \cdot & var(\hat{\theta}) & cov(\hat{\theta},\hat{\lambda}) \\ \cdot & \cdot & \cdot & var(\hat{\lambda}) \end{bmatrix}.$$

Hence, the $100(1-\delta)\%$ asymptotic confidence intervals (ACIs) for each φ_k is given by

$$ACI_k = \left[\hat{\varphi}_k - Z_{\frac{\delta}{2}}\sqrt{\hat{I}_{kk}}, \hat{\varphi}_k + Z_{\frac{\delta}{2}}\sqrt{\hat{I}_{kk}}\right],$$

where $\hat{I}_{kk}$ is the (k,k) diagonal elements of $I_n(\hat{\varphi})^{-1}$ for $k = 1, 2, 3, 4$ and $Z_{\frac{\delta}{2}}$ is the upper δ^{th} percentile of the standard normal distribution.

B. MLE FOR RIGHT-CENSORED DATA

In the same way, we have established the log-likelihood function of the MEW model for data that has been right-censored. Let (y_i, δ_i), where i ranges from $i = 1, 2, \ldots, n$, be a random sample that has been censored. For $\delta_i = 1$, y_i is a failure or survival time, and for $\delta_i = 0$, y_i is a censored time. We can express the log-likelihood function of the MEW model in this case as:

$$\ell_C(\boldsymbol{\varphi}) = \sum_{i=1}^{n}\delta_i\log f(y_i) + \sum_{i=1}^{n}(1-\delta_i)\log R(y_i)$$
$$= \nu\log\left(\gamma\theta^{-\gamma}\right) + (\gamma-1)\sum_{i=1}^{n}\delta_i\log y_i + \sum_{i=1}^{n}\delta_i(y_i/\theta)^{\gamma} + \sum_{i=1}^{n}\delta_i\log c_i - \lambda\sum_{i=1}^{n}a_i - \sum_{i=1}^{n}a_i^{\alpha},$$

where a_i and c_i are given in (9), $\nu = \sum_{i=1}^{n}\delta_i$, and $f(.)$ and $S(.)$ are the PDF (3) and survival function (4). The estimate $\widehat{\boldsymbol{\varphi}} = \left(\widehat{\alpha}, \widehat{\gamma}, \widehat{\lambda}, \widehat{\theta}\right)'$ of $(\alpha, \gamma, \lambda, \theta)'$ can be obtained using the log-likelihood function (10) via a similar approach with the non-censored case in Section IV-A.

C. PERCENTILE BOOTSTRAP CONFIDENCE INTERVALS FOR MEW PARAMETERS

Finding the standard error of a point estimator with a complex form is either challenging or even not achievable with standard statistical methodology. In such a circumstance, the bootstrap method may be employed (see [45]). To implement the bootstrap method, we generate bootstrap samples from $f(t; \widehat{\boldsymbol{\varphi}})$, where $\widehat{\boldsymbol{\varphi}}$ is the ML estimate of $\boldsymbol{\varphi}$, and compute a bootstrap estimate $\widehat{\boldsymbol{\varphi}}_*$ (the ML estimate of $\boldsymbol{\varphi}$ calculated from the bootstrap sample). This technique is known as the parametric bootstrap. Besides, we can apply the non-parametric bootstrap when the density function $f(t; \widehat{\boldsymbol{\varphi}})$ is not available or difficult to generate data. In this circumstance, we treat the original real data as the population and draw bootstrap samples with replacement from it. This process is repeated B times as describe in the following steps.

Step 1 Produce a bootstrap sample 1: $t_1^1, t_2^1, \ldots, t_n^1$ from the given data set sampled with replacement to compute the ML estimate of $\boldsymbol{\varphi}$, say $\widehat{\boldsymbol{\varphi}}_* = (\widehat{\alpha}_*^1, \widehat{\gamma}_*^1, \widehat{\lambda}_*^1, \widehat{\theta}_*^1)'$.

Step 2 Repeat **step 1** B times to obtain the bootstrap samples set for the estimates.

Step 3 Then use the bootstrap samples to compute the bootstrap sample means $\bar{\widehat{\boldsymbol{\varphi}}}_* = (\bar{\widehat{\alpha}}_*, \bar{\widehat{\gamma}}_*, \bar{\widehat{\lambda}}_*, \bar{\widehat{\theta}}_*)'$ and

standard error $SE_{B_p}(\bar{\bar{\boldsymbol{\varphi}}}_*) = \left(SE_{B_p}(\bar{\bar{\alpha}}_*), SE_{B_p}(\bar{\bar{\gamma}}_*), SE_{B_p}(\bar{\bar{\lambda}}_*), SE_{B_p}(\bar{\bar{\theta}}_*)\right)'$ using the standard methods.

Step 4 Let $\bar{\bar{\alpha}}_*^{\delta}$ represent the δ percentile of $\hat{\alpha}_*^j$, for $j = 1, 2, \ldots, B$. That is

$$\frac{1}{B}\sum_{j=1}^{B} I_{\left\{\hat{\alpha}_*^j \le \bar{\bar{\alpha}}_*^{\delta}\right\}} = \delta, \quad 0 < \delta < 1,$$

where $I_{\{.\}}$ is the standard indicator function. Thus, the $(1-\xi)\%$ bootstrap confidence interval (CL_{Bp}) for α is defined as

$$\left(\bar{\bar{\alpha}}_{*(\xi/2)}, \bar{\bar{\alpha}}_{*(1-\xi/2)}\right)$$

Step 5 Repeat **steps 4** to obtain the $(1-\xi)\%$ CL_{Bp} for γ, λ, and θ.

D. BAYESIAN ESTIMATION

Bayesian inference is a different approach from frequentist inference that has been widely used in many fields to estimate parameters, especially in complex situations. This article suggests using the Bayesian paradigm to estimate the parameters of the MEW model (more information can be found in [46] and [47]). The Bayesian model is constructed by the product of the likelihood function and prior distribution $\pi(\boldsymbol{\varphi})$ for $\boldsymbol{\varphi} = (\gamma, \alpha, \theta, \lambda)'$, which derived the posterior distribution of $\boldsymbol{\varphi}$ represented by $\phi(\boldsymbol{\varphi}|\mathcal{D})$. $\pi(\boldsymbol{\varphi})$ denoted the distribution of $\boldsymbol{\varphi}$ before observing the data $D : t_1, t_2, \ldots, t_n$. Based on the Bayes theorem, we can obtained the distribution of the posterior as $\boldsymbol{\varphi}|\mathcal{D}$ defined:

$$\pi(\boldsymbol{\varphi}|\mathcal{D}) = \frac{\mathcal{L}(\mathcal{D}|\boldsymbol{\varphi})\pi(\boldsymbol{\varphi})}{\int_{\boldsymbol{\Theta}} \mathcal{L}(\mathcal{D}|\varphi)\pi(\boldsymbol{\varphi})d\boldsymbol{\varphi}} \propto \mathcal{L}(\mathcal{D}|\boldsymbol{\varphi})\pi(\boldsymbol{\varphi}), \tag{10}$$

where $\int_{\Theta} \mathcal{L}(\mathcal{D}|\boldsymbol{\varphi})\phi(\boldsymbol{\varphi})d\boldsymbol{\varphi}$ is the normalizing constant of the posterior distribution of $\boldsymbol{\varphi}$, $\boldsymbol{\Theta}$ is the parameter space, and $\mathcal{L}(\mathcal{D}|\boldsymbol{\varphi})$ represents the likelihood function of MEW distribution, and is given by

$$\mathcal{L}(\mathcal{D}|\boldsymbol{\varphi}) = \frac{\gamma^n}{\theta^n}\mathcal{A}_i \exp\left\{\lambda\sum_{i=1}^{n}\mathcal{B}_i - \sum_{i=1}^{n}(e^{(t_i/\theta)^{\gamma}} - 1)^{\alpha} + \sum_{i=1}^{n}(t_i/\theta)^{\gamma} + (\gamma-1)\sum_{i=1}^{n}\log(t_i/\theta)\right\}, \tag{11}$$

where $\mathcal{A}_i = \prod_{i=1}^{n}\left[\lambda + \alpha(e^{(t_i/\theta)^{\gamma}} - 1)^{\alpha-1}\right]$ and $\mathcal{B}_i = 1 - e^{(t_i/\theta)^{\gamma}}$.

In this study, the parameters γ, α, θ, and λ are supposed to have gamma priors following the works of Kundu Howlader [48], Soliman et al. [49], and Abba and Wang [29]. Let $\pi(\varphi_k)$ denote the gamma prior having (ν_k, γ_k) as the hyper-parameters, with PDF given by

$$\pi(\varphi_k) = \frac{\nu_k^{\gamma_k}}{\gamma(\gamma_k)}\varphi_k^{\gamma_k-1}e^{-\nu_k\varphi_k}, \quad \nu_k > 0, \gamma_k > 0, \quad k = 1, 2, 3, 4. \tag{12}$$

Thus, $\gamma \sim \pi(\gamma|\nu_1, \gamma_1)$, $\alpha \sim \pi(\alpha|\nu_2, \gamma_2)$, $\theta \sim \pi(\theta|\nu_3, \gamma_3)$ and $\lambda \sim \pi(\lambda|\nu_4, \gamma_4)$. For this study, we assigned the hyper-parameter values which yield means approximate to the MLEs of the parameters [27]. The joint posterior distribution of $\boldsymbol{\varphi}|\mathcal{D}$ is therefore obtained after substituting Eq.(11)-(12) into (13) as

$$\pi(\boldsymbol{\varphi}|\mathcal{D}) \propto \frac{\gamma^{n+\gamma_1-1}\alpha^{\gamma_2-1}\lambda^{\gamma_4-1}}{\theta^{n-\gamma_3+1}}\mathcal{A}_i \exp\{-\alpha_1\gamma - \alpha_2\alpha - \alpha_3\theta - \alpha_4\lambda\} \times \exp\left\{\lambda\sum_{i=1}^{n}\mathcal{B}_i - \sum_{i=1}^{n}(e^{(t_i/\theta)^{\gamma}} - 1)^{\alpha} + \sum_{i=1}^{n}(t_i/\theta)^{\gamma} + (\gamma-1)\sum_{i=1}^{n}\log(t_i/\theta)\right\}. \tag{13}$$

We can determined the marginal posterior densities from (12) for the γ, α, θ, and λ as

$$\pi(\gamma|\mathcal{D}) \propto \gamma^{n+\gamma_1-1}\mathcal{A}_i \exp\left\{+(\gamma-1)\sum_{i=1}^{n}\log(t_i/\theta) - \alpha_1\gamma\right\} \times \exp\left\{\lambda\sum_{i=1}^{n}\mathcal{B}_i - \sum_{i=1}^{n}(e^{(t_i/\theta)^{\gamma}} - 1)^{\alpha} + \sum_{i=1}^{n}(t_i/\theta)^{\gamma}\right\},$$

$$\pi(\alpha|\mathcal{D}) \propto \alpha^{\gamma_2-1}\mathcal{A}_i \exp\left\{-\sum_{i=1}^{n}(e^{(t_i/\theta)^{\gamma}} - 1)^{\alpha} - \alpha_2\alpha\right\}$$

$$\pi(\theta|\mathcal{D}) \propto \theta^{-n+\gamma_3-1}\mathcal{A}_i \exp\left\{(\gamma-1)\sum_{i=1}^{n}\log(t_i/\theta) - \alpha_3\theta\right\} \times \exp\left\{\lambda\sum_{i=1}^{n}\mathcal{B}_i - \sum_{i=1}^{n}(e^{(t_i/\theta)^{\gamma}} - 1)^{\alpha} + \sum_{i=1}^{n}(t_i/\theta)^{\gamma}\right\},$$

$$\pi(\lambda|\mathcal{D}) \propto \lambda^{\gamma_4-1}\mathcal{A}_i \exp\left\{\lambda\sum_{i=1}^{n}\mathcal{B}_i - \alpha_4\lambda\right\}. \tag{14}$$

Applying the square error loss function (SELF), the Bayes estimators of $\gamma, \alpha, \theta, \lambda$, survival function $R(t)$, and HRF $h(t)$, are derived as follows:

$$\begin{aligned}
\hat{\gamma}_* &= \mathbb{E}(\gamma|\mathcal{D}) = \int_{\Theta}\gamma\pi(\boldsymbol{\varphi}|\mathcal{D})\mathrm{d}\boldsymbol{\varphi}\\
\hat{\alpha}_* &= \mathbb{E}(\alpha|\mathcal{D}) = \int_{\Theta}\alpha\pi(\boldsymbol{\varphi}|\mathcal{D})\mathrm{d}\boldsymbol{\varphi}\\
\hat{\theta}_* &= \mathbb{E}(\theta|\mathcal{D}) = \int_{\Theta}\theta\pi(\boldsymbol{\varphi}|\mathcal{D})\mathrm{d}\boldsymbol{\varphi}\\
\hat{\lambda}_* &= \mathbb{E}(\lambda|\mathcal{D}) = \int_{\Theta}\lambda\pi(\boldsymbol{\varphi}|\mathcal{D})\mathrm{d}\boldsymbol{\varphi}\\
\hat{R}_* &= \mathbb{E}(R(t;\boldsymbol{\varphi})|\mathcal{D}) = \int_{\Theta}R(t;\boldsymbol{\varphi})\pi(\boldsymbol{\varphi}|\mathcal{D})\mathrm{d}\boldsymbol{\varphi}\\
\hat{h}_* &= \mathbb{E}(h(t;\boldsymbol{\varphi})|\mathcal{D}) = \int_{\Theta}h(t;\boldsymbol{\varphi})\pi(\boldsymbol{\varphi}|\mathcal{D})\mathrm{d}\boldsymbol{\varphi}
\end{aligned} \tag{15}$$

Calculating the Bayes estimates (BEs) via the posterior means may be infeasible with no closed-form solutions of the marginal posterior densities $\pi(\alpha|\mathcal{D})$, $\pi(\gamma|\mathcal{D})$, $\pi(\lambda|\mathcal{D})$, and $\pi(\theta|\mathcal{D})$. Hence, we opt for NUTS [50], another form of the HMC algorithm, to samples from the posterior distribution using `Rstan` [51] in `R`. A recent re-explanation of the HMC algorithm can be found in [29].

Hence, for a posterior sample $\{\varphi_s, s = 1, 2, \ldots, N\}$ generated from $\pi(\boldsymbol{\varphi}|\mathcal{D})$, the approximate Bayes estimates of MEW parameters α, γ, λ, and θ, as well as the reliability function $S(t)$ and HRF $h(t)$ are calculated as

$$\widehat{\gamma}_* \approx \frac{1}{N-\wp}\sum_{s=\wp+1}^{N}\gamma_s$$
$$\widehat{\alpha}_* \approx \frac{1}{N-\wp}\sum_{s=\wp+1}^{N}\alpha_s$$
$$\widehat{\lambda}_* \approx \frac{1}{N-\wp}\sum_{s=\wp+1}^{N}\lambda_s$$
$$\widehat{\theta}_* \approx \frac{1}{N-\wp}\sum_{s=\wp+1}^{N}\theta_s$$
$$\widehat{R}_*(t) \approx \frac{1}{N-\wp}\sum_{s=\wp+1}^{N}S(t;\varphi_s)$$
$$\widehat{h}_*(t) \approx \frac{1}{N-\wp}\sum_{s=\wp+1}^{N}h(t;\varphi_s),$$

where $\wp$ represents the number of burn-in observations/ iterations prior to stationarity of the samples. It is highly advisable to run the simulation for m parallel chains ($m = 3, 4$ or 5) for better assessment of the sampler convergence [25]. Therefore, we can proceed to compute the posterior means for m parallel chains as follows:

$$\widehat{\alpha}_* \approx \frac{1}{m(N-\wp)}\sum_{b=1}^{m}\sum_{s=\wp+1}^{N}\alpha_{(s,b)}$$
$$\widehat{\gamma}_* \approx \frac{1}{m(N-\wp)}\sum_{b=1}^{m}\sum_{s=\wp+1}^{N}\gamma_{(s,b)}$$
$$\widehat{\lambda}_* \approx \frac{1}{m(N-\wp)}\sum_{b=1}^{m}\sum_{s=\wp+1}^{N}\lambda_{(s,b)}$$
$$\widehat{\theta}_* \approx \frac{1}{m(N-\wp)}\sum_{b=1}^{m}\sum_{s=\wp+1}^{N}\theta_{(s,b)}$$
$$\widehat{R}_*(t) \approx \frac{1}{m(N-\wp)}\sum_{b=1}^{m}\sum_{s=\wp+1}^{N}S(t;\varphi_{s,b})$$
$$\widehat{h}_*(t) \approx \frac{1}{m(N-\wp)}\sum_{b=1}^{m}\sum_{s=\wp+1}^{N}h(t;\varphi_{s,b}).$$

We checked the nature of the convergence of the HMC samples for each chain by considering the Gelman and Rubin's [52] potential scale reduction factor (PSRF, $\widehat{R}$). The PSRF is a combination of Between-chain and Within-chain variances, and the HMC sample is considered to be converged if $\widehat{R}$ is less than 1.1. To calculate the $(1-\delta)100\%$ Bayesian credible intervals (BCIs) for the parameters, we sorted the HMC samples in ascending order as $\varphi_{k,1} \leq \varphi_{k,2} \leq \cdots \leq \varphi_{k,N-s}$, where k ranges from $k = 1, \ldots, 4$, and expressed the intervals as $[\varphi_{k,\frac{\delta}{2}(N-s)}, \varphi_{k,(1-\frac{\delta}{2})(N-s)}]$. Additionally, we computed the approximate $(1-\delta)100\%$ highest posterior density (HPD) interval of μ_k, which is the interval consisting the highest posterior density.

E. SIMULATION RESULTS

Simulation studies involve using computer experiments to create data through random sampling. This allows us to gain insight into the behavior of statistical techniques, as we have knowledge of parameters used in generating the data. This understanding helps us examine the properties of methods, such as bias. Reference [53] provides further information on simulation studies.

In this section, we conduct a Monte Carlo simulation experiment to assess the effectiveness of the suggested estimators using the proposed maximum likelihood and Bayesian methodologies for estimating MEW parameters. The parameters were estimated using the simulated samples produced via the sampling procedure described in Section III-A, and under different parameter values and 1000 samples for ten sample sizes, $n = 30, 60, \ldots, 270$, and 300. To compute the Bayes estimates, we consider 1000 iterations under gamma priors with hyper-parameter values derived from the selected MEW parameter values. We count out the first 50% as warm-up samples.

We performed all the simulations and computations in `R4.2.2` software using `nlminb` package, an `R` base package.

The estimates of bias and mean square error (MSE) were considered to assess the performance of the two methods. FIGUREs 5 - 6(a)-(d) provides the visual views of the simulation results for various parameter sets and different sample sizes.As n rises, both the biases and MSEs for the ML and Bayes estimates approach zero, which explains the consistency of the suggested approaches. The line plots in FIGUREs 5 - 6(a)-(d) reveal that bias and MSE estimations under the ML approach are, in most cases, quite small compared to the Bayesian method. Therefore, the proposed estimation methodologies can be implemented for diverse MEW distribution scenarios.

V. APPLICATIONS OF MEW MODEL TO CENSORED AND UNCENSORED DATA

In this section, we examine the potential difference of the enhanced MEW model with other methodologies, including the EW [11], AddW [12], exponentiated modified Weibull extension (EMWE) [54], exponentiated AddW (EaddW) [55], and GExtEW [13] distributions on two failure time data.

For the two illustrations, the parameter estimates of all models were determined using the ML methodology, whereas we use Bayesian method to obtain the posterior summaries of the MEW parameters. We similarly reports the $-\ell$, AIC, BIC, and KS goodness-of-fit statistics for comparative inferences.

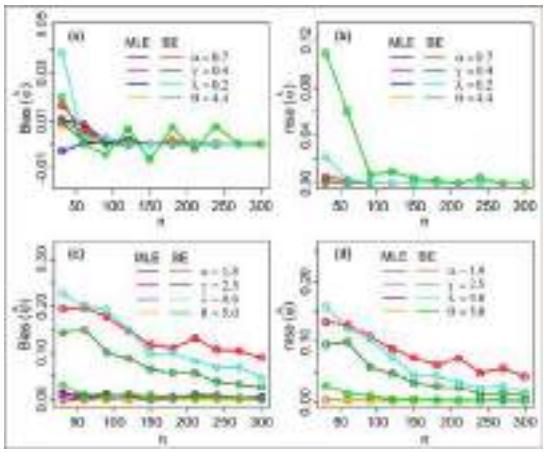

FIGURE 5. Simulation findings for ML and Bayesian methods under different settings of parameters: (a)-(b) for $\alpha = 0.7$, $\gamma = 0.4$, $\lambda = 0.2$, and $\theta = 4.4$ and (c)-(d) for $\alpha = 1.8$, $\gamma = 2.5 =$, $\lambda = 0.8$, and $\theta = 5$.

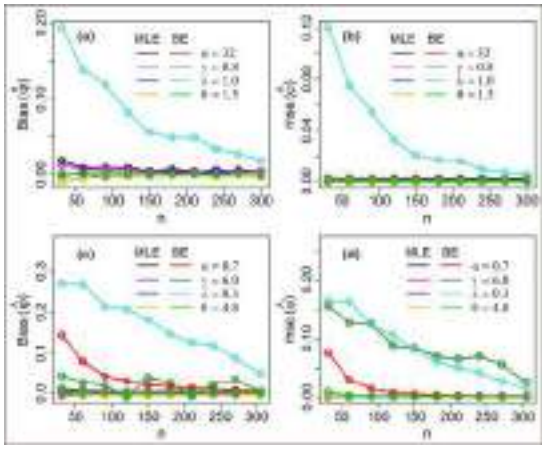

FIGURE 6. Simulation findings for ML and Bayesian methods under different settings of parameters: (a)-(b) for $\alpha = 32$, $\gamma = 0.8$, $\lambda = 1$, and $\theta = 1.5$, and (c)-(d) for $\alpha = 0.7$, $\gamma = 6$, $\lambda = 0.3$, and $\theta = 4.8$.

Besides that, the HRF and survival function curves for the trained models are employed to further support the comparisons. We gives the Bayes estimate and their associated 95% HPD intervals for the MEW parameters, along with their respective trace plots, density plots, box plots, and scatted plot matrix from the HMC output.

A. FAILURE AND RUNNING TIMES OF 30 DEVICES

The data represent the failure and running times (FRTs) of thirty devices reported by Meeker et al. [21], which is characterized by bathtub-shaped HR. Although, the data is well-known as a benchmark for evaluating the adequacy of fit for models with bathtub-shaped HRF (see for instance, [13], [28], [33]), most of the existing literature applied it an uncensored data by ignoring the censoring indicator. However, this study used the FRT data in it full scale as censored. TABLE 5 present the data, where the '*' represent the censoring indicator. The FRTs is reported to have two failure modes: electric surge and wear-out, and therefore matched the physical interpretation of MEW model. Hence, the enhanced

TABLE 5. Failure and running times, consisting of failure and running times of 30 devices. Where '*' is a right-censored indicator.

275	13	147	23	181	30
65	10	300*	173	106	300*
300*	212	300*	300*	300*	2.0
261	293	88	247	28	143
300*	23	300*	80	245	266

TABLE 6. ML estimates along with parametric and non-parametric goodness-of-fits statistics; Censored FRT data of devices.

Model	$\hat{\gamma}$	$\hat{\alpha}$	$\hat{\theta}$	$\hat{\lambda}$	$\hat{\beta}$	$-\ell$	AIC	BIC	KS	p-value
3-parameters										
EW		0.8327		0.0035	0.0016	142.641	291.282	295.486	0.2960	0.0104
4-parameters										
AddW	0.6340	1.0150	0.0805	0.0028		162.394	332.787	338.392	0.5137	$2.7e^{-7}$
EMWE	0.1061	204.40		$9.6e^{-7}$	4.5290	142.479	292.957	298.562	0.2636	0.0309
MEW	6.9430	0.1091	339.040	0.7538		140.659	289.319	294.923	0.2629	0.0317
5-parameters										
EaddW	3.1919	1.0475	0.0579	0.0031	99.472	142.247	294.494	301.500	0.2904	0.0127
GExEW	0.1098	1.5812	0.7917	0.0017	6.3465	142.189	294.377	301.383	0.2895	0.0131

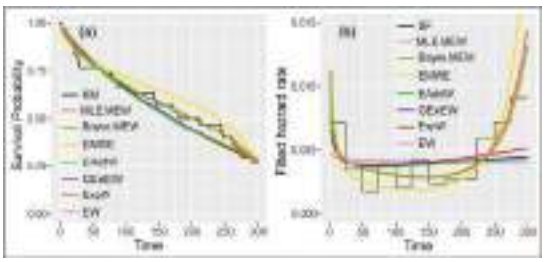

FIGURE 7. Curves of the fitted hazard rate and survival functions for MEW and other competing models; Censored FRT data of devices.

model is suitable for fitting the FRTs. Table 6 presents the ML estimates, negative log-likelihood ($-\ell$), AIC, BIC, and AICc values for various trained distributions, including MEW. Based on the table, the MEW model has the lowest negative log-likelihood ($-\ell$), surpassing the other fitted models by a significant margin of at least one unit. Moreover, the MEW model outperforms all the other learned additive and non-additive models, as evidenced by its top ranking in terms of AIC, AICc, and BIC selection criteria. This implies that the proposed MEW model is the most appropriate for accurately describing the FRT data. FIGURE 7(a)-(b) shows the fitted models' survival functions and HRFs. In FIGURE 7(a), the reliability curves of the learned models and the Kaplan-Meier (KM) estimate are depicted. It is obvious that the fitted reliability curves of MEW approximates the KM to some reasonable degree better than the competing models. It is observed from FIGURE 7(b) that the HRF of the MEW has provided the best curves that resemble the FRTs non-parametric HR represented by the empirical step function (SF).

To proceed with the Bayesian inference, we construct the posterior samples of the parameters for the data by employing the HMC algorithm and generating four parallel chains, each with 2000 independently and identically observations. We discard the first 1000 as warm-up and managed the last 1000 posterior samples to calculate the posterior summaries given in TABLE 7. FIGURE 8(a)-(c) depicts the trace, posterior density and box plots of the HMC-generated samples. The trace plots reveal the four parallel HMC chains converge to comparatively the same target distribution for each of the

TABLE 7. ML and Bayes estimates, along with 95% ACI, B_pCI and HPD intervals for MEW parameters; Censored FRT data of devices.

Parameter	ML estimate	95% ACI	95% B_pCI	Bayes estimate	95% HPD
γ	6.9430	[6.9338, 6.9522]	[4.2164, 6.9430]	6.9441	[6.8454, 7.0355]
α	0.1091	[0.0635, 0.1548]	[0.1046, 0.2243]	0.1098	[0.0669, 0.1554]
θ	339.04	[339.038, 339.042]	[339.040 339.042]	339.00	[337.33, 340.48]
λ	0.7538	[0.0000, 1.7264]	[0.7538, 2.9648]	0.6721	[0.0070, 1.4375]

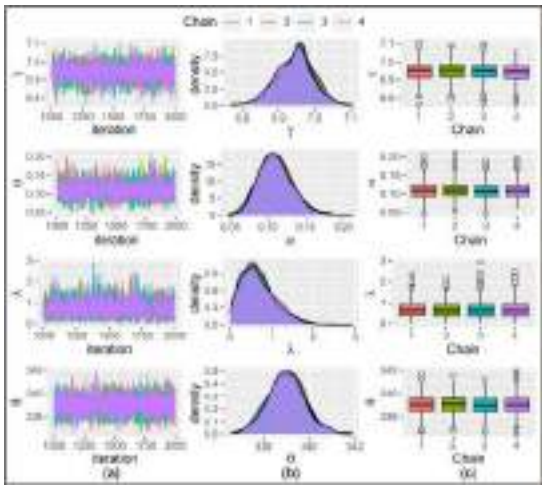

FIGURE 8. Posterior plots depicting: (a) the trace plots (b) density curves and (c) box plots for the MEW parameters; Censored FRT data of devices.

four parameters. This finding is also supported by the density and box plots which are nearly symmetrically distributed around the central values. The correlations between the Bayes estimates of the parameters are shown in scatter matrix given in FIGURE 9. The fact that most parameter pairs appear to have very low correlation points to the accuracy of the posterior estimates under the HMC method.

TABLE 7 provides the ML, Bayes estimates and 95% intervals of α, γ, λ, and θ. From the Table, the values of estimated values for the first three parameters α, γ and θ of the proposed MEW are nearly close to each other under the two approaches. However, the Bayes estimate of λ is shown to be relatively bigger than its ML estimate. We also display the survival and HR curves of the Bayesian MEW model in FIGURE 8, which are depicted to strongly agreed with their MLE counterparts.

Thus, we conclude that the numerical results are consistent with FIGUREs 8-7, and that the MEW model may be applied to analyze and predict the reliability of the censored failure and running time of devices via either of the estimation approaches.

B. TIME TO FAILURE OF 50 DEVICES

The values in TABLE 8 correspond to the times to failure (TTF) of 50 electronic devices [56]. The TTF data is still one of the most well-known benchmark lifetime data, distinguished by bathtub-shape HR and used to validate the fits of a newly built model. It has been used by Mudholkar and Srivastava [57], Xie and Lai [12], Sarhan and Apaloo [54], EL-Baset and Ghazal [55], and Shakhatreh et al. [13] to

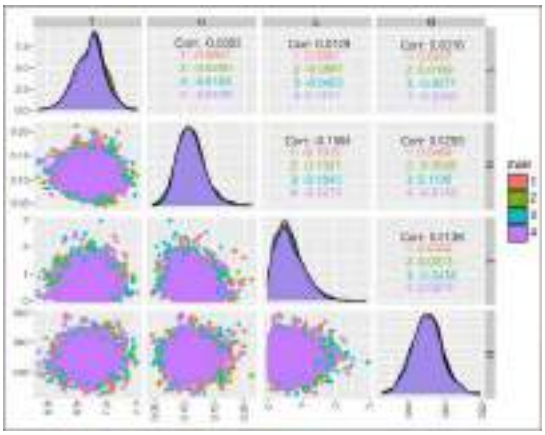

FIGURE 9. Scatter plot matrix of HMC output for fitting MEW; Censored FRT data of devices.

TABLE 8. Time to failure of 50 electronic devices.

0.1	0.2	1.0	1.0	1.0	1.0	1.0	2.0	3.0	6.0
7.0	11	12	18	18	18	18	18	21	32
36	40	45	46	47	50	55	60	63	63
67	67	67	67	72	75	79	82	82	83
84	84	84	85	85	85	85	85	86	86

TABLE 9. ML estimates along with parametric and non-parametric goodness-of-fits statistics; TTF data.

Model	$\hat{\gamma}$	$\hat{\alpha}$	$\hat{\theta}$	$\hat{\lambda}$	$\hat{\beta}$	$\hat{\ell}$	AIC	BIC	KS	p-value
3-parameters										
EW		0.3735		0.0186	0.0405	239.484	484.968	490.705	0.1941	0.0462
4-parameters										
AddW	1.622×10^{-8}	4.134	0.090	0.461		221.714	451.427	459.075	0.126	0.4073
EMWE	3.165	7.020×10^{-5}	49.206		0.144	213.816	435.632	443.280	0.140	0.2832
MEW	0.622	95.49	153.1	1.297		205.052	418.1033	425.751	0.098	0.7243
5-parameters										
EAddW	5.368×10^{-15}	7.541	4.902	0.056	345.18	215.855	441.711	451.271	0.119	0.4783
GExtEW	0.088	34.029	0.508	0.003	0.128	221.587	453.173	462.733	0.151	0.2035

validate the fit of ExpW, AddW, EMWE, EaddW, and GExtEW models, respectively. The outcomes from each study show how these models outperform the other competing models analyzed in the studies. In this illustration, we will show that the MEW model can better fit TTF data than the earlier mentioned and many recently introduced models.

TABLE 9 lists the ML estimates for all the trained models' parameters, along with their associated model selection criteria. It is noted that AIC = 418.103, BIC = 425.751, and KS = 0.098 for the enhanced MEW model is by far the least among all other competing models. Consequently, the MEW provides the best fit among all other distributions. FIGURE 10(a)-(b) demonstrates the curves of the fitted survival and HRF for the MEW, EMWE, EaddW, GExtEW, ExpW, and EW models for TTF data fitting, along with their corresponding empirical survival and HR step function (SF). As shown by FIGURE 10(a), the MLE.MEW survival curve best resembles the Kaplan-Meier SF (KM) among all the fitted survival curves. The MEW is also shown to explore the HR of the TTF data best than the other distributions. It can be further seen from FIGURE 10(b) that the HR curve of the MEW model has identified the early, constant/random, and wear-out segments of the empirical SF. This is very significant among all the HR curves of the models.

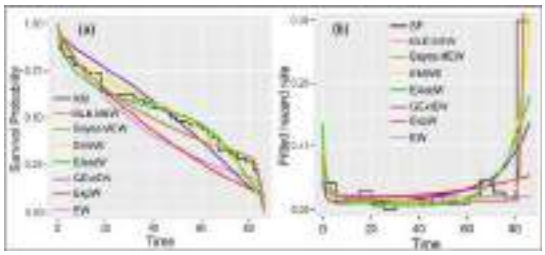

FIGURE 10. Curves of the fitted hazard rate and survival functions for MEW and other competing models; TTF of electronic devices.

TABLE 10. ML and Bayes estimates, along with 95% ACI, B_pCI and HPD intervals for MEW parameters; TTF of electronic devices.

Parameter	ML estimate	95% ACI	95% B_pCI	Bayes estimate	95% HPD
γ	0.6220	[0.6049, 0.6387]	[0.6127, 0.6276]	0.6220	[0.6121, 0.6318]
α	95.490	[77.508, 113.47]	[95.491, 95.491]	95.026	[78.057, 111.14]
θ	153.13	[151.77, 154.50]	[153.14, 153.14]	153.15	[152.01 154.39]
λ	1.2972	[0.8762, 1.7172]	[1.0178, 1.8645]	1.2973	[1.0179, 1.6086]

To determine the Bayes estimate of MEW parameters, we sampled 2000 observations from the proposed posterior distributions of the parameters for four parallel chains. In each case, the last 1000 samples are recorded for posterior computations while leaving out the first 1000 observations as a warm-up.

FIGURE 12 depicts the trace plots, posterior density curves, and box plots generated by the HMC method. For each parameter, the trace plots reveal the quick convergence of all four parallel chains to the same target distribution. The density curves and box plots have supported the trace plot by displaying the approximately symmetrically distributed curves around the mid-values and plots with similar properties. We further present the scatter matrix of the posterior samples as given in FIGURE 11, to show the less sensitivity of the HMC algorithm to correlated parameters. The figure reveals that all pairs of MEW parameters have very weak relationships except for the correlation between γ and θ. Therefore, it depicts how the algorithm could attenuate the correlation effect while producing decent posterior samples.

TABLE 10 displays the ML and Bayes estimates of γ, α, θ, and λ, along with their 95% asymptotic, bootstrap and HPD intervals. From the Table, all the estimated values from either approaches are very close to each other. The intervals have well contained the their associated estimates.

Consequently, we can infer that the MEW model under the two inferential methodologies have well describe the TTF data as evidently shown by the numerical and pictorial findings.

C. COMPATIBILITY OF THE MEW MODEL

Here, we will discuss how well the proposed MEW model matches with two data sets through a straightforward but logical method called predictive simulation [58]. The basic concept behind using predictive simulation to evaluate the compatibility of the model is to compare the original sample or its relevant function with the data generated by the fitted model, which is referred to as the predictive sample. To accomplish this, we will employ box plots, a commonly used visual comparison tool, to evaluate the predictive samples from the fitted MEW models (using the two estimated approaches) with each of the original data sets.

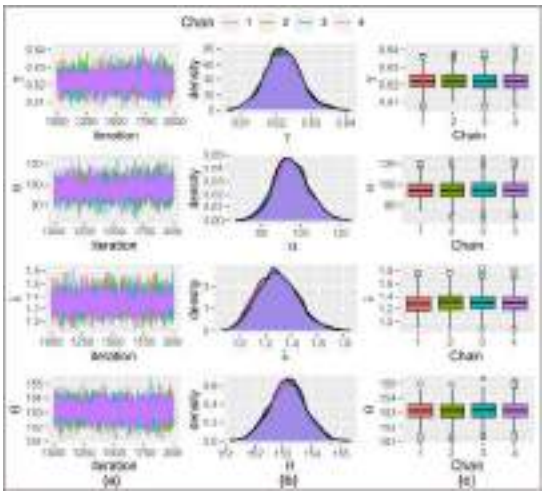

FIGURE 11. Posterior plots depicting: (a) the trace plots (b) density curves and (c) box plots for the MEW parameters; TTF of electronic devices.

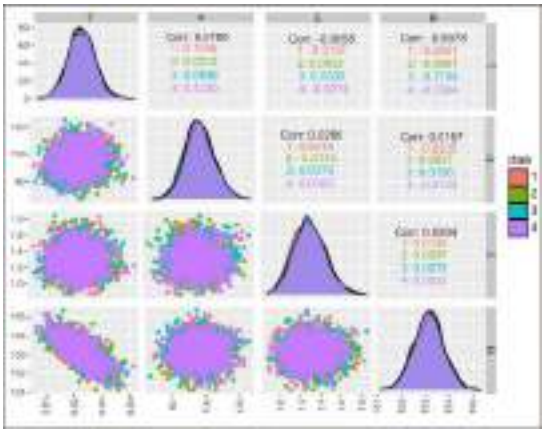

FIGURE 12. Scatter plot matrix of HMC output for fitting MEW; TTF of electronic devices.

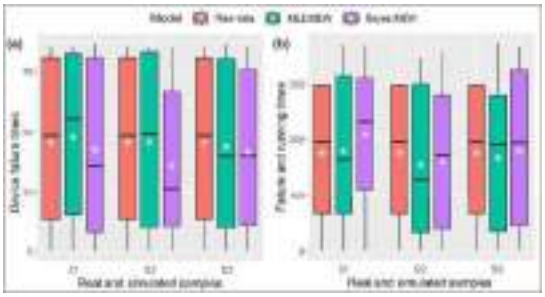

FIGURE 13. Box plots for the original data and three distinct simulated samples (S1, S2 and S3) from the trained MEW models under Bayesian and ML approaches: (a) Meeker-Escobar (FRT) data and (b) Aarset (TTF) data. Asterisk (*) within the bars represent the sample means.

The figures in FIGURE 13 display box plots that compare three predictive samples from MLE.MEW and Bayes. MEW to the original sample (Real data) for the two examples. It is evident from the box plots that the predictive samples from the learned MEW using both estimation methods are in better agreement with the original sample in all cases. These results indicate that the MEW distribution closely matches the experimental data distributions. Based on numerical and graphical analyses, the proposed MEW model provides a more accurate description of the Meeker-Escobar and Aarset data sets than the other five competing models. As a result, the MEW model is highly recommended for studying and predicting failure time data sets with different bathtub failure rates in the fields of reliability engineering and survival studies, among others.

VI. CONCLUSION

We introduce a modified version of the exponential-Weibull (EW) distribution, named the modified exponential-Weibull (MEW) model, which extended some physical character of the EW. We conduct a thorough Bayesian inference of the MEW model and also present the maximum likelihood method. To sample from the MEW posterior distribution, we use the Hamiltonian Monte Carlo algorithm. We assess the performance of the MEW model by applying it to two sets of data on the failure times of devices, one with censored and one with uncensored data, both exhibiting a bathtub-shaped hazard rate. We compare the MEW model to six other bathtub-shaped methodologies, including the EW, AddW, EMWE, EAddW, and GExEW models based on the hazard rate characterizations of the data. We present model selection criteria, survival, and hazard rate curves for each model to determine which model best fits the case study data. Our numerical and graphical results suggest that the MEW model may be the most suitable for describing the failure times of the devices. Thus, our findings indicate that modifying the EW model while preserving its physical interpretation is the optimal approach to extending the model.

APPENDIX. ELEMENTS OF INFORMATION MATRIX

$$\frac{\partial^2 \ell(\varphi)}{\partial \lambda^2} = -c_i^{-2},$$

$$\frac{\partial^2 \ell(\varphi)}{\partial \alpha \partial \lambda} = \frac{a_i^{\alpha-1}(1+\alpha\log(a_i))}{c_i^2},$$

$$\frac{\partial^2 \ell(\varphi)}{\partial \lambda \partial \theta} = -\frac{\gamma}{\theta}(1-\alpha(\alpha-1)a_i^{\alpha-2}c_i^{-2})b_i,$$

$$\frac{\partial^2 \ell(\varphi)}{\partial \lambda \partial \gamma} = (1-\alpha(\alpha-1)a_i^{\alpha-2}c_i^{-2})b_i\log(x_i/\theta),$$

$$\frac{\partial^2 \ell(\varphi)}{\partial \alpha^2} = (2+\alpha\log(a_i))\,a_i^{\alpha-1}\frac{\log(a_i)}{c_i} - a_i^{2(\alpha-1)}\left(\frac{1+\log(a_i)}{c}\right)^2 + a_i^{\alpha}\log^2(a_i),$$

$$\frac{\partial^2 \ell(\varphi)}{\partial \alpha \partial \gamma} = -\alpha(\alpha-1)(1+\alpha\log(a_i))\frac{b_i}{a_i c_i^2}a_i^{2(\alpha-1)}\log(x_i/\theta) + \frac{b_i}{a_i c_i}a_i^{\alpha-1}[\alpha+(\alpha-1)(1+\alpha\log(a_i))]\log(x_i/\theta) + (1+\alpha\log(a_i))\frac{b_i}{a_i}a_i^{\alpha}\log(x_i/\theta),$$

$$\frac{\partial^2 \ell(\varphi)}{\partial \alpha \partial \theta} = \frac{\gamma(\alpha-1)}{\theta}(1+\alpha\log(a_i))\frac{b_i}{a_i c_i^2}a_i^{2(\alpha-1)} - \frac{\gamma}{\theta}(1+\alpha\log(a_i))\frac{b_i}{a_i}a_i^{\alpha} - \frac{\gamma}{\theta}[1+(\alpha-1)(1+\alpha\log(a_i))]\frac{b_i}{a_i}a_i^{\alpha-1},$$

$$\frac{\partial^2 \ell(\varphi)}{\partial \theta^2} = \frac{n\gamma}{\theta^2} + \frac{\gamma\alpha(\alpha-1)}{\theta^2} \times \left[\frac{1}{a_i} + \gamma\left(\frac{\alpha-1}{a_i} + (x/\theta)^{\gamma}+1\right) - \alpha\gamma(\alpha-1)\frac{a_i^{\alpha-3}b_i}{c_i}\right]\frac{a_i^{\alpha}b_i}{a_i c_i} + \frac{\gamma^2\lambda}{\theta^2}\left[\frac{1}{\gamma}+1+(x_i/\theta)^{\gamma}\right]b_i + \frac{\gamma^2\alpha}{\theta^2}\left[\frac{1}{\gamma}+1+(x_i/\theta)^{\gamma}+\frac{(\alpha-1)}{a_i}\right]\frac{a_i^{\alpha}b_i}{a_i} + \frac{\gamma^2}{\theta^2}\left[\frac{1}{\gamma}+1+(x/\theta)^{\gamma}-\frac{b_i}{a_i+1}\right]\frac{b_i}{a_i+1},$$

$$\frac{\partial^2 \ell(\varphi)}{\partial \gamma^2} = -\frac{n}{\gamma^2} + \alpha(\alpha-1) \times \left[\left(1+(x_i/\theta)^{\gamma}+(\alpha-2)\frac{b_i}{a_i}\right)c_i - \alpha(\alpha-1)a_i^{\alpha-2}b_i\right] \times a_i^{\alpha}b_i\left(\frac{\log(x_i/\theta)}{a_i c_i}\right)^2 - \lambda(1+(x_i/\theta)^{\gamma})b_i\log^2(x_i/\theta) - \alpha\left[1+(x_i/\theta)^{\gamma}+(\alpha-1)\frac{b_i}{a_i}\right] \times a_i^{\alpha-1}b_i\log^2(x_i/\theta) + b_i\left(\frac{\log(x_i/\theta)}{a_i+1}\right)^2\left[(a_i+1)(1+(x_i/\theta)^{\gamma})-b_i\right],$$

$$\frac{\partial^2 \ell(\varphi)}{\partial \theta \partial \gamma} = -\frac{n}{\theta} - \frac{\gamma\lambda}{\theta} \times \left[\frac{a_i^{\alpha}b_i}{a_i^2 c_i} + \gamma\left[\left(1+(x_i/\theta)^{\gamma}+(\alpha-2)\frac{b_i}{a_i}\right)c_i - \alpha(\alpha-1)a_i^{\alpha-2}b_i\right]\right] \times \frac{a_i^{\alpha}b_i}{a_i^2 c_i^2}\log(x_i/\theta) - \frac{\alpha}{\theta}\left[b_i a_i^{\alpha-1} + \gamma\left[1+(x_i/\theta)^{\gamma}+(\alpha-1)\frac{b_i}{a_i}\right]\right.$$

$$\times a_i^{\alpha-1} b_i \log(x_i/\theta)\Big] - \frac{1}{\theta}\left[1+\gamma\frac{\log(x_i/\theta)}{(a_i+1)} \times \left[(a_i+1)(1+(x_i/\theta)^{\gamma})-b_i\right]\right]\frac{b_1}{a_i+1} - \frac{\lambda}{\theta}\left[1+\gamma(1+(x_i/\theta)^{\gamma})\log(x_i/\theta)\right]b_i,$$

where $a_i = e^{(x_i/\theta)^{\gamma}} - 1$, $b_i = (x_i/\theta)^{\gamma} e^{(x_i/\theta)^{\gamma}}$, and $c_i = \lambda + \alpha a_i^{\alpha-1}$.

ACKNOWLEDGMENT

Princess Nourah bint Abdulrahman University Researchers Supporting Project number (PNURSP2023R443), Princess Nourah bint Abdulrahman University, Riyadh, Saudi Arabia.

REFERENCES

[1] S. K. Upadhyay, A. Gupta, and D. K. Dey, "Bayesian modeling of bathtub shaped hazard rate using various Weibull extensions and related issues of model selection," *Sankhya B*, vol. 74, no. 1, pp. 15–43, May 2012.

[2] A. Singh and S. Adachi, "Bathtub curves and pipe prioritization based on failure rate," *Built Environ. Project Asset Manag.*, vol. 3, no. 1, pp. 105–122, Jul. 2013.

[3] D. Krishnachaitanya, A. Chitra, and S. Biswas, "Reliability approach for the power semiconductor devices in EV applications," in *Artificial Intelligent Techniques for Electric and Hybrid Electric Vehicles*. Wiley, 2020, pp. 115–124, doi: 10.1002/9781119682035.ch6.

[4] J. P. Poletto, "An alternative to the exponential and Weibull reliability models," *IEEE Access*, vol. 10, pp. 118759–118778, 2022.

[5] N. S. H. Kumar, R. P. Choudhary, and C. S. Murthy, "Reliability-based analysis of probability density function and failure rate of the shovel–dumper system in a surface coal mine," *Model. Earth Syst. Environ.*, vol. 7, no. 3, pp. 1727–1738, Sep. 2021.

[6] L. Fan, Z. Hu, Q. Ling, H. Li, H. Qi, and H. Chen, "Reliability analysis of computed tomography equipment using the q-Weibull distribution," *Eng. Rep.*, vol. 5, Jan. 2023, Art. no. e12613.

[7] L. C. Méndez-González, L. A. Rodríguez-Picón, I. J. C. Pérez-Olguin, V. Garcia, and A. E. Quezada-Carreón, "A reliability analysis for electronic devices under an extension of exponentiated perks distribution," *Qual. Rel. Eng. Int.*, vol. 39, no. 3, pp. 776–795, Apr. 2023.

[8] L. C. Méndez-González, L. A. Rodríguez-Picón, D. J. Valles-Rosales, R. Romero-López, and A. E. Quezada-Carreón, "Reliability analysis for electronic devices using beta-Weibull distribution," *Qual. Rel. Eng. Int.*, vol. 33, no. 8, pp. 2521–2530, Dec. 2017.

[9] Y.-J. Yang, W. Wang, X.-Y. Zhang, Y.-L. Xiong, and G.-H. Wang, "Lifetime data modelling and reliability analysis based on modified Weibull extension distribution and Bayesian approach," *J. Mech. Sci. Technol.*, vol. 32, no. 11, pp. 5121–5126, Nov. 2018.

[10] G. Klutke, P. C. Kiessler, and M. A. Wortman, "A critical look at the bathtub curve," *IEEE Trans. Rel.*, vol. 52, no. 1, pp. 125–129, Mar. 2003.

[11] G. M. Cordeiro, E. M. Ortega, and A. J. Lemonte, "The exponential-Weibull lifetime distribution," *J. Stat. Comput. Simul.*, vol. 84, no. 12, pp. 2592–2606, 2014.

[12] M. Xie and C. D. Lai, "Reliability analysis using an additive Weibull model with bathtub-shaped failure rate function," *Rel. Eng. Syst. Saf.*, vol. 52, no. 1, pp. 87–93, Apr. 1996.

[13] M. K. Shakhatreh, A. J. Lemonte, and G. M. Cordeiro, "On the generalized extended exponential-Weibull distribution: Properties and different methods of estimation," *Int. J. Comput. Math.*, vol. 97, no. 5, pp. 1029–1057, May 2020.

[14] C. Lai, M. Xie, and D. Murthy, "Bathtub shaped failure rate life distributions," in *Handbook of Statistics*, vol. 20. 2001, ch. 3, pp. 69–104.

[15] M. K. Shakhatreh, A. J. Lemonte, and G. Moreno-Arenas, "The log-normal modified Weibull distribution and its reliability implications," *Rel. Eng. Syst. Saf.*, vol. 188, pp. 6–22, Aug. 2019.

[16] A. Saboor, M. Kamal, and M. Ahmad, "The transmuted exponential-Weibull distribution with applications," *Pak. J. Statist.*, vol. 31, no. 2, pp. 229–250, 2015.

[17] G. M. Cordeiro, A. Saboor, M. N. Khan, O. Gamze, and M. A. Pascoa, "The Kumaraswamy exponential-Weibull distribution: Theory and applications," *Hacettepe J. Math. Statist.*, vol. 45, no. 4, pp. 1203–1229, 2016.

[18] T. Pogány and A. Saboor, "The gamma exponentiated exponential-Weibull distribution," *Filomat*, vol. 30, no. 12, pp. 3159–3170, 2016.

[19] Z. Tang, W. Zhou, J. Zhao, D. Wang, L. Zhang, H. Liu, Y. Yang, and C. Zhou, "Comparison of the Weibull and the crow-AMSAA model in prediction of early cable joint failures," *IEEE Trans. Power Del.*, vol. 30, no. 6, pp. 2410–2418, Dec. 2015.

[20] Z. Tang, C. Zhou, W. Jiang, W. Zhou, X. Jing, J. Yu, B. Alkali, and B. Sheng, "Analysis of significant factors on cable failure using the Cox proportional hazard model," *IEEE Trans. Power Del.*, vol. 29, no. 2, pp. 951–957, Apr. 2014.

[21] W. Q. Meeker, L. A. Escobar, and F. G. Pascual, *Statistical Methods for Reliability Data*. Hoboken, NJ, USA: Wiley, 2022.

[22] S. J. Almalki and J. Yuan, "A new modified Weibull distribution," *Rel. Eng. Syst. Saf.*, vol. 111, pp. 164–170, Mar. 2013.

[23] B. He, W. Cui, and X. Du, "An additive modified Weibull distribution," *Rel. Eng. Syst. Saf.*, vol. 145, pp. 28–37, Jan. 2016.

[24] A. Asgharzadeh, S. Nadarajah, and F. Sharafi, "Weibull Lindley distribution," *Revstat-Stat. J.*, vol. 16, no. 1, pp. 87–113, 2018.

[25] T. T. Thach and R. Bris, "Improved new modified Weibull distribution: A Bayes study using Hamiltonian Monte Carlo simulation," *Proc. Inst. Mech. Eng., O, J. Risk Rel.*, vol. 234, no. 3, pp. 496–511, Jun. 2020.

[26] B. Tarvirdizade and M. Ahmadpour, "A new extension of Chen distribution with applications to lifetime data," *Commun. Math. Statist.*, vol. 9, no. 1, pp. 23–38, Mar. 2021.

[27] T. T. Thach and R. Bris, "An additive Chen–Weibull distribution and its applications in reliability modeling," *Qual. Rel. Eng. Int.*, vol. 37, no. 1, pp. 352–373, Feb. 2021.

[28] B. Abba, H. Wang, and H. S. Bakouch, "A reliability and survival model for one and two failure modes system with applications to complete and censored datasets," *Rel. Eng. Syst. Saf.*, vol. 223, Jul. 2022, Art. no. 108460.

[29] B. Abba and H. Wang, "A new failure times model for one and two failure modes system: A Bayesian study with Hamiltonian Monte Carlo simulation," *Proc. Inst. Mech. Eng., O, J. Risk Rel.*, vol. 237, Jan. 2023, Art. no. 1748006X2211463.

[30] K. Cooray, "Generalization of the Weibull distribution: The odd Weibull family," *Stat. Model.*, vol. 6, no. 3, pp. 265–277, Oct. 2006.

[31] M. Bourguignon, R. B. Silva, and G. M. Cordeiro, "The Weibull-G family of probability distributions," *J. Data Sci.*, vol. 12, no. 1, pp. 53–68, Mar. 2021.

[32] M. Xie, Y. Tang, and T. N. Goh, "A modified Weibull extension with bathtub-shaped failure rate function," *Rel. Eng. Syst. Saf.*, vol. 76, no. 3, pp. 279–285, Jun. 2002.

[33] H. Wang, B. Abba, and J. Pan, "Classical and Bayesian estimations of improved Weibull–Weibull distribution for complete and censored failure times data," *Appl. Stochastic Models Bus. Ind.*, vol. 38, no. 6, pp. 997–1018, Nov. 2022.

[34] R. E. Glaser, "Bathtub and related failure rate characterizations," *J. Amer. Stat. Assoc.*, vol. 75, no. 371, pp. 667–672, Sep. 1980.

[35] I. Aswin, P. Sankaran, and S. Sunoj, "The bilinear mean residual quantile function," *Commun. Statist.-Theory Methods*, vol. 51, pp. 1–15, Feb. 2022.

[36] A. S. Krishnan, S. M. Sunoj, and P. G. Sankaran, "Quantile-based reliability aspects of cumulative Tsallis entropy in past lifetime," *Metrika*, vol. 82, no. 1, pp. 17–38, Jan. 2019.

[37] N. U. Nair and P. G. Sankaran, "Quantile-based reliability analysis," *Commun. Statist.-Theory Methods*, vol. 38, no. 2, pp. 222–232, Jan. 2009.

[38] W.-J. Huang and N.-C. Su, "Characterizations of distributions based on moments of residual life," *Commun. Statist.-Theory Methods*, vol. 41, no. 15, pp. 2750–2761, Aug. 2012.

[39] M. Xie, T. N. Goh, and Y. Tang, "On changing points of mean residual life and failure rate function for some generalized Weibull distributions," *Rel. Eng. Syst. Saf.*, vol. 84, no. 3, pp. 293–299, Jun. 2004. [Online]. Available: https://www.sciencedirect.com/science/article/pii/S0951832003002862

[40] R. C. Gupta and S. Kirmani, "Residual life function in reliability studies," in *Frontiers in Reliability*. Singapore: World Scientific, 1998, pp. 175–190.

[41] G. Casella and R. L. Berger, *Statistical Inference*. Pacific Grove, CA, USA: Brooks/Cole, 1990.

[42] R. B. Millar, *Maximum Likelihood Estimation and Inference: With Examples in R, SAS and ADMB*. Hoboken, NJ, USA: Wiley, 2011.

[43] A. Henningsen and O. Toomet, "MaxLik: A package for maximum likelihood estimation in R," *Comput. Statist.*, vol. 26, no. 3, pp. 443–458, Sep. 2011.
[44] G. Casella and R. L. Berger, *Statistical Inference*. Boston, MA, USA: Cengage, 2021.
[45] R. J. Tibshirani and B. Efron, "An introduction to the bootstrap," *Monographs Statist. Appl. Probab.*, vol. 57, no. 1, pp. 33–48, 1993.
[46] J. G. Ibrahim, M.-H. Chen, D. Sinha, J. Ibrahim, and M. Chen, *Bayesian Survival Analysis*, vol. 2. Berlin, Germany: Springer, 2001.
[47] C. P. Robert, *The Bayesian Choice: From Decision-Theoretic Foundations to Computational Implementation*, vol. 2. Berlin, Germany: Springer, 2007.
[48] D. Kundu and H. Howlader, "Bayesian inference and prediction of the inverse Weibull distribution for type-II censored data," *Comput. Statist. Data Anal.*, vol. 54, no. 6, pp. 1547–1558, Jun. 2010.
[49] A. A. Soliman, A. H. Abd-Ellah, N. A. Abou-Elheggag, and E. A. Ahmed, "Modified Weibull model: A Bayes study using MCMC approach based on progressive censoring data," *Rel. Eng. Syst. Saf.*, vol. 100, pp. 48–57, Apr. 2012.
[50] M. D. Homan and A. Gelman, "The No-U-Turn sampler: Adaptively setting path lengths in Hamiltonian Monte Carlo," *J. Mach. Learn. Res.*, vol. 15, no. 1, pp. 1593–1623, Jan. 2014.
[51] Stan Development Team. *RStan: The R Interface to Stan*. Accessed: Jan. 5, 2023. [Online]. Available: http://mc-stan.org/rstan/
[52] A. Gelman and D. B. Rubin, "Inference from iterative simulation using multiple sequences," *Stat. Sci.*, vol. 7, no. 4, pp. 457–472, Nov. 1992.
[53] T. P. Morris, I. R. White, and M. J. Crowther, "Using simulation studies to evaluate statistical methods," *Statist. Med.*, vol. 38, no. 11, pp. 2074–2102, May 2019.
[54] A. M. Sarhan and J. Apaloo, "Exponentiated modified Weibull extension distribution," *Rel. Eng. Syst. Saf.*, vol. 112, pp. 137–144, Apr. 2013.
[55] A. E.-B.-A. Ahmad and M. G. M. Ghazal, "Exponentiated additive Weibull distribution," *Rel. Eng. Syst. Saf.*, vol. 193, Jan. 2020, Art. no. 106663.
[56] M. V. Aarset, "How to identify a bathtub hazard rate," *IEEE Trans. Rel.*, vol. R-36, no. 1, pp. 106–108, Apr. 1987.
[57] G. S. Mudholkar and D. K. Srivastava, "Exponentiated Weibull family for analyzing bathtub failure-rate data," *IEEE Trans. Rel.*, vol. 42, no. 2, pp. 299–302, Jun. 1993.
[58] A. Gupta, B. Mukherjee, and S. K. Upadhyay, "Weibull extension model: A Bayes study using Markov chain Monte Carlo simulation," *Rel. Eng. Syst. Saf.*, vol. 93, no. 10, pp. 1434–1443, Oct. 2008.

LAILA A. AL-ESSA received the Ph.D. degree from Princess Noura bint Abdulrahman University, Saudi Arabia. She is currently an Assistant Professor of mathematics with the Department of Mathematical Sciences, College of Science, Princess Noura bint Abdulrahman University. Her research interests include reliability functions, estimation problems, and ordinal statistics.

MUSTAPHA MUHAMMAD received the B.Sc. degree in mathematics from Bayero University, Kano, Nigeria, the M.Sc. degree in mathematics from the Jordan University of Science and Technology, Jordan, the National Diploma degree in mechanical engineering from the School of Technology, Kano State Polytechnic, Nigeria, in 2007, and the Ph.D. degree in applied mathematics from the School of Mathematical Sciences, Hebei Normal University, China. Since 2014, he has been with the Department of Mathematics, Northwest University Kano, Nigeria, then with the Department of Mathematical Sciences, Bayero University. He is currently a Lecturer with the Department of Mathematics, Guangdong University of Petrochemical Technology, China. He has published several articles in an international peer reviewed journals. His research interests include distribution theory, regression modeling, R programming, statistical mechanics, Bayesian statistics, reliability, stochastic, and estimation.

M. H. TAHIR received the M.Sc. and Ph.D. degrees in statistics from The Islamia University of Bahawalpur (IUB), Pakistan, in 1990 and 2010, respectively. He has been teaching with the Department of Statistics, IUB, since 1992. He is currently a Professor of Statistics, and the Chairs of the Department of Statistics and Dean, Faculty of Computing, IUB. His current research interests include the generalized classes of distributions and their special models, compounded and modified models, reliability and survival analysis, data science, AI and machine learning tools. He has produced more than 70 M.Phil. and 10 Ph.D. He has more than 100 international publications in his credit. He is also reviewer of more than 50 international journals related to these fields.

BADAMASI ABBA received the B.Sc. degree in statistics from the Kano University of Science and Technology, Wudil, Nigeria, in 2014, and the M.Sc. degree in statistics from Ahmadu Bello University, Zaria, Nigeria, in 2017. He is currently pursuing the Ph.D. degree in applied statistics with Central South University, Changsha, China. Some of his articles have been published in high-impact journals. His current research interests include survival analysis, reliability analysis, distribution theory, and Bayesian analysis.

JINSEN XIAO received the B.Sc. degree in mathematics from the Guangdong University of Petrochemical Technology, Maoming, China, in 2007, and the M.Sc. and Ph.D. degrees in mathematics from Guangzhou University, Guangzhou, China, in 2010 and 2013, respectively. He is currently an Associate Professor with the Department of Mathematical, Guangdong University of Petrochemical Technology. He has published several articles appeared in international peer-reviewed journals, and presided several projects under research funds, including the Natural Science Foundation of Guangdong Province and the National Natural Science foundation of China. His research interests include harmonic analysis and differential equations.

FARRUKH JAMAL received the M.Sc. and M.Phil. degrees in statistics from The Islamia University of Bahawalpur (IUB), Punjab, Pakistan, in 2003 and 2006, respectively, and the Ph.D. degree from IUB under the supervision of Dr. M. H. Tahir. Before joining S.A. College in 2012, he was a Statistical Officer with the Agriculture Department, from 2007 to 2012. He is currently an Assistant Professor with the Department of Statistics, IUB. He has 200 publications in his credit.